INTERACTION NOTES

NOTE 467

JUNE 1988

Slot Apertures Having Depth Described By Local Transmission Line Theory

Larry K. Warne and Kenneth C. Chen

Sandia National Laboratories, Albuquerque, NM 87185

ABSTRACT

The problem of electromagnetic penetration of a narrow slot aperture in a thick conducting plane is considered when the conductivity of the plane (and slot walls) is large but not necessarily infinite and when somewhat lossy gaskets are placed in the slot. The length of the slot and the wavelength are assumed to be much larger than the slot cross section. The conducting plane surface impedance is assumed to be small compared to the impedance of free space, and the thickness of the plane is assumed to be much larger than the skin depth to prevent direct penetration. The wavelength and skin depth in the gasket material are assumed to be much larger than the gasket cross section. The problem is partitioned into a

"local" region, where transmission line theory is used to describe the antenna modes along the slot, and a "nonlocal" region, where a filament type integral representation is used. The result is a modified Hallén type integro–differential equation for the slot voltage (or magnetic current). The local transmission line theory allows the effects of wall loss and gaskets to be included in a simple and intuitive manner. Examples involving a rectangular slot aperture are given. The finite conductivity of the conducting plane, even for good conductors, reduces the penetration when realistic slot dimensions are used. Gaskets, even with relatively small loss tangents, also reduce the penetration when realistic slot dimensions are used.

ACKNOWLEDGEMENT

The authors wish to thank T. E. Koontz, Sandia National Laboratories, who prepared the numerical figures.

I. INTRODUCTION

A previous paper [1] considered electromagnetic penetration of narrow slot apertures in thick, perfectly conducting planes. This paper gives an alternative, more powerful formulation. This new formulation is also applicable when the conducting plane (and slot wall) conductivity is large but not necessarily infinite and when somewhat lossy gaskets are introduced into the slot. Restrictions on the slot parameters are given below to ensure that the transverse slot voltage remains nearly constant over the local cross section.

A simple derivation is given of a general integro–differential equation for the voltage (or magnetic current) distribution along a narrow slot aperture. The length of the slot ℓ and the wavelength λ are assumed to be much larger than the long dimension of the slot cross section characterized by s, where

$$\ell, \lambda >> s \quad . \tag{1}$$

Figure 1 shows a typical cross section. The conducting plane has thickness d.

The lossless case without gasket type material in the slot is reduced to the solution of Hallén's integral equation with an equivalent antenna radius.

Conducting plane and wall materials that are not perfectly conducting are considered. The skin depth of the wall material δ is assumed to be much smaller than d to prevent direct penetration of the conducting plane. The surface impedance Z_s of the wall material is assumed to be small compared to the impedance of free space η_o. Furthermore, for the purpose of evaluation of the transmission line parameters, it is assumed that the axial (along the long dimension of the slot ℓ) voltage drops caused by this wall impedance are

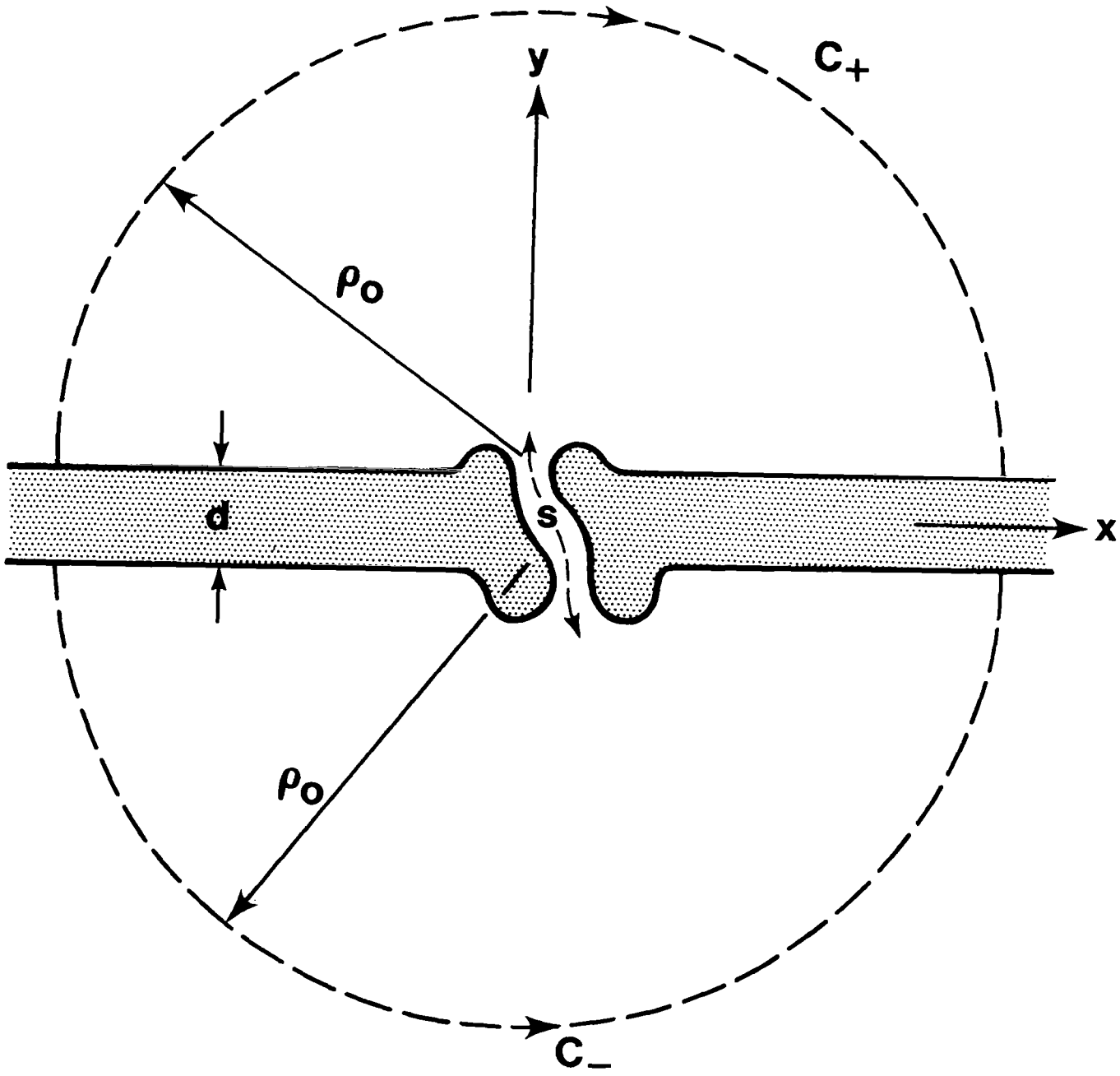

Figure 1. Slot aperture cross section and the local region.

small compared to the inductive voltage drops (typical transmission line perturbation theory). This last condition can be relaxed if the surface current density is sufficiently uniform, as discussed in example 3 of section III. Note, as discussed in the example, that further restrictions on the parameters are required when this last condition is relaxed.

The case is treated in which the slot is filled with somewhat lossy gaskets. The skin depth in the gasket material δ_g and the wavelength in the gasket material λ_g are assumed to be much larger than the cross sectional gasket dimensions. Transverse diffusion may thus be neglected.

Several examples, involving a rectangular slot aperture of width w and depth d, are given to illustrate the effect of wall loss and gaskets on the voltage distribution and the transmitted power.

II. GENERAL INTEGRO–DIFFERENTIAL EQUATION

The slot cross sectional geometry is shown in Figure 1. A distance ρ_o is chosen such that

$$\ell, \lambda >> \rho_o >> s \ . \tag{2}$$

The distance ρ_o defines a local region as shown in Figure 1. It is measured from $y = \pm \frac{d}{2}$ and roughly the slot center $x = 0$. It is assumed that any gasket material is contained within the local region and that ρ_o is much larger than the gasket dimensions.

A plane electromagnetic wave is incident from the half space $y < -\frac{d}{2}$. We are interested in antenna modes supported by the slot. The important incident field component is directed along the long dimension of the slot ℓ

$$H_z^{inc} = H_{oz}\, e^{i\underline{k} \cdot \underline{r}} \ , \tag{3}$$

where $\underline{k}$ is the wave vector, $\underline{r}$ is the position vector, and H_{oz} is the incident magnetic field amplitude in the z direction; harmonic time dependence $e^{-i\omega t}$ is used throughout. Because of condition (1) the incident field in the vicinity of the slot is approximately

$$H_z^{inc} = H_{oz}\, e^{ikz\cos\theta_o} \ , \tag{4}$$

where $k = \omega\sqrt{\epsilon_o \mu_o}$ is the magnitude of the wavevector or wavenumber, ω is the radian frequency, ϵ_o is the electric permittivity of free space, μ_o is the magnetic permeability of free space, and θ_o is the angle the incident wave vector makes with the positive z axis. A reflected wave is generated by the presence of the conducting plane at $y = -\frac{d}{2}$. Because of condition (1), the short circuit axial magnetic field is approximately

$$H_z^{sc} \approx 2\, H_z^{inc} \,. \tag{5}$$

Because of condition (2), the axial magnetic field scattered by the slot, in the nonlocal region, can be written approximately as

$$H_z^{>}(\rho,z) = \frac{i}{\omega\mu_o}\left(\frac{\partial^2}{\partial z^2} + k^2\right) \int_{-h}^{h} G(\rho,z,z')\, \underline{I}_m^{+}(z')\, dz' \;,$$

$$y \gtrless \pm \frac{d}{2} \;, \tag{6}$$

where $\ell = 2h$, and ρ is a cylindrical coordinate measured from $x = 0$ and $y = \pm \frac{d}{2}$; the sign depending on which particular half space is being considered ($H_z^{>}$ is the nonlocal slot axial magnetic field for $\rho > \rho_o$). The total magnetic current $\underline{I}_m^{+}$ is defined by

$$\underline{I}_m^{+} = 2 \int_{C_{\pm}} K_{mz}\, d\ell \;,\; y \gtrless \pm \frac{d}{2} \;, \tag{7}$$

where the contours $C_{\pm}$ are the cylindrical contours at radius ρ_o (shown in Figure 1) and K_{mz} is the axial component of the magnetic surface current density. The magnetic surface current density is related to the discontinuity in electric field at a surface by means of [2]

$$\underline{K}_m = -\,\underline{n} \times (\underline{E}_2 - \underline{E}_1) \;, \tag{8}$$

where the surface is the boundary between region 1 and region 2 and the unit normal $\underline{n}$ points from region 1 to region 2. Relation (8) can be used to short the slot by placing perfect conductors at the boundaries $C_{\pm}$ with magnetic surface currents introduced to yield

the proper tangential electric fields. The total magnetic current can thus be written in terms of the voltage across the slot defined by

$$V_{\pm} = \int_{C_{\pm}} \underline{E} \cdot \underline{d\ell} \ , \ y \gtrless \pm \frac{d}{2} \ , \tag{9}$$

where the positive reference of the voltage is on the left ($x < 0$) conductor ($C_{\pm}$ extend from the left to the right conductor). The relation is given by

$$I_m^{\pm} = \pm 2 \, V_{\pm} \ , \tag{10}$$

where, because of the conditions stated in the introduction, $V_+ \approx V_- \approx V$.

The Green's function in (6) is given by

$$G(\rho,z,z') = \frac{e^{i\,kR}}{4\pi R} \ , \tag{11}$$

where $$R = \sqrt{\rho^2 + (z - z')^2} \ .$$

Note that the radius ρ_o at which the magnetic current is placed is reduced to zero in (6). This is the usual filament approximation [3] and is permitted by condition (2).

Maxwell's equations in integral form are now applied to contours in the local region analogous to standard transmission line theory [4]. Figure 2a shows the contour for the equation

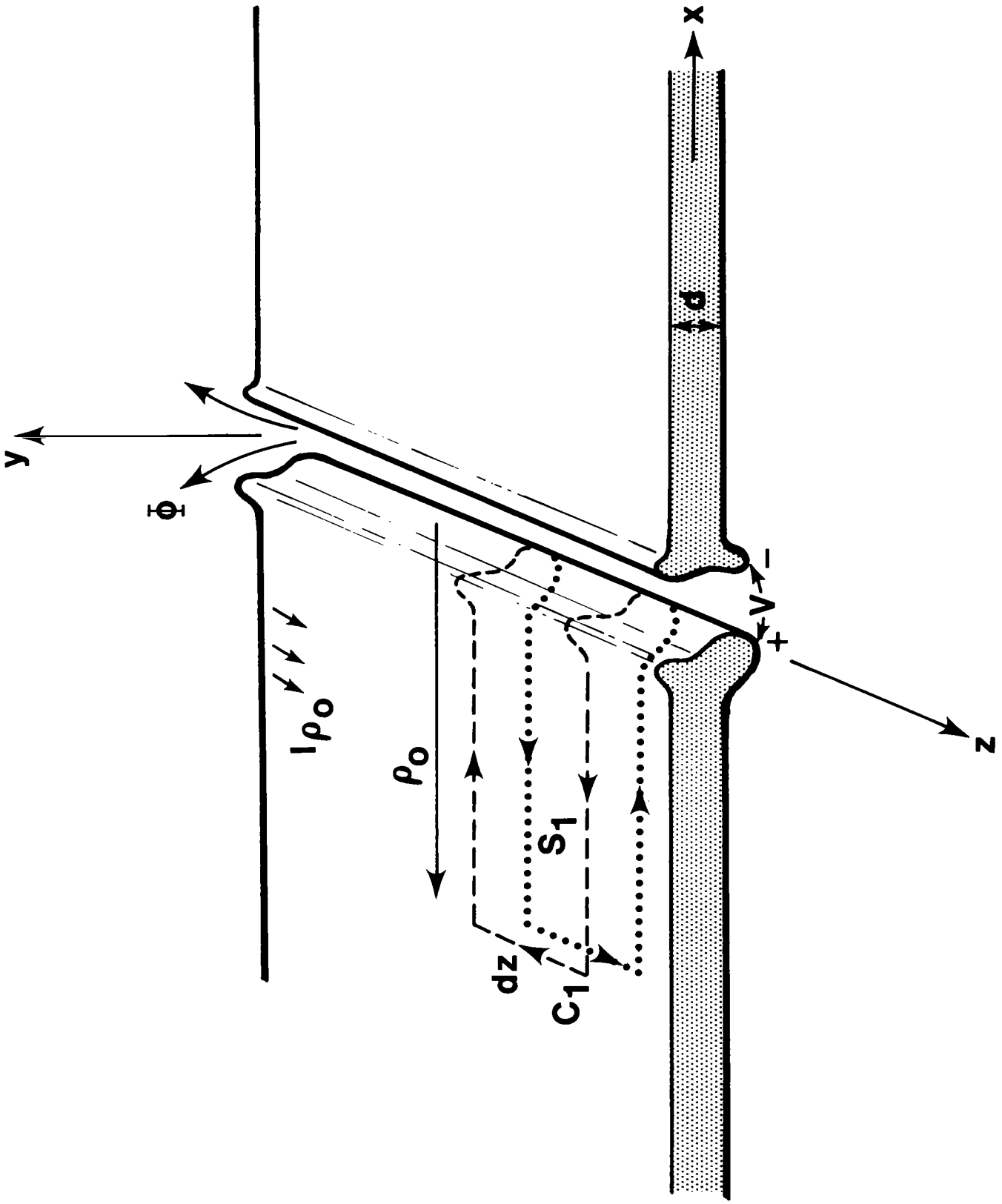

Figure 2. (a) Contour C_1 for application of Maxwell–Ampere–Ohm law.

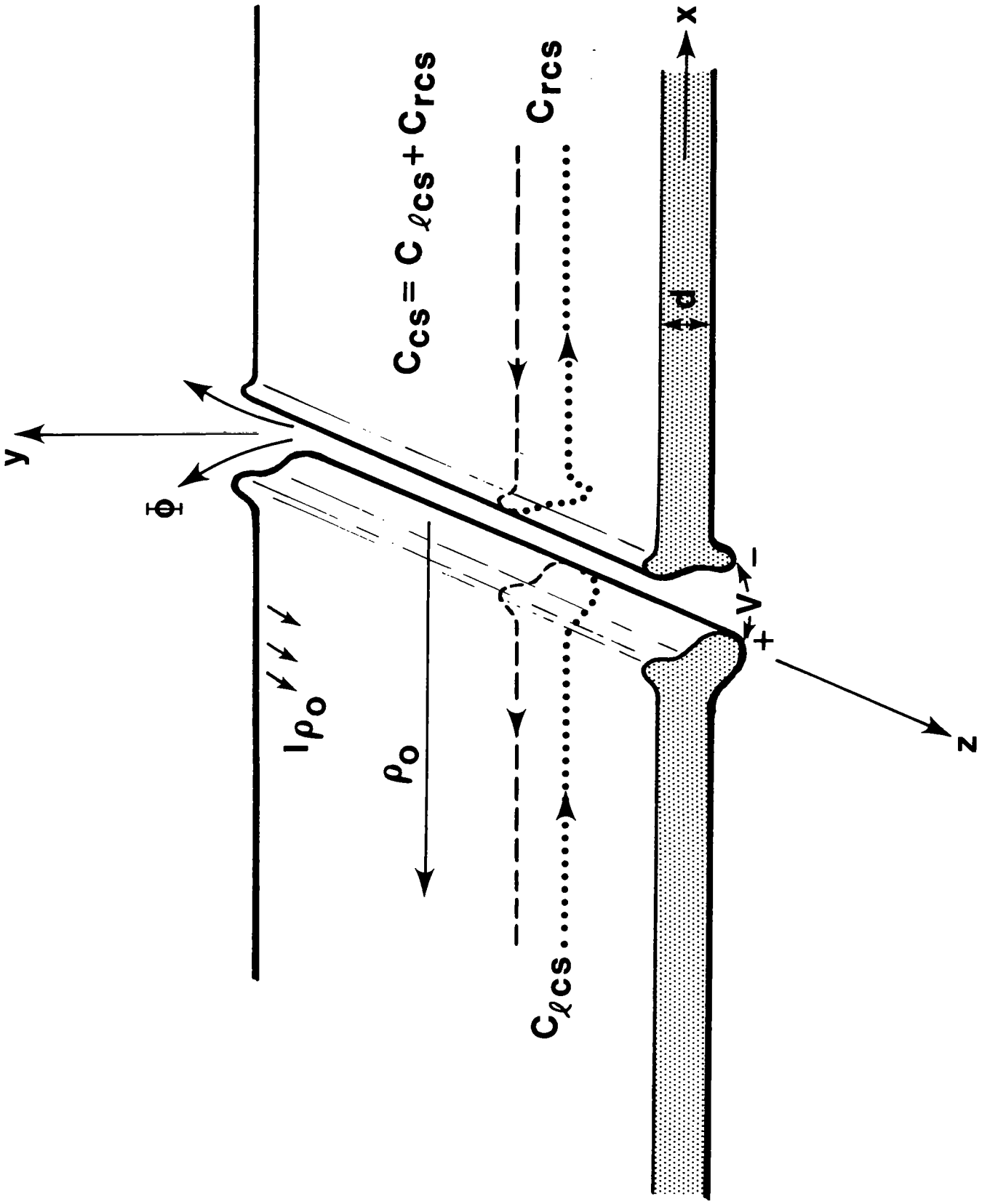

(b) Definition of cross section contour C_{cs}.

$$\oint_{C_1} \underline{H} \cdot \underline{d\ell} = \int_{S_1} (\sigma_g \underline{E} - i\omega \underline{D}) \cdot \underline{n}\, dS \ , \qquad (12)$$

where σ_g is the electric conductivity of the gasket material.

Note that the transverse components of the incident fields will be ignored in (12) and also in (18). These components contribute to the much smaller transverse dipole moments of the slot [5] and have little influence on the antenna problem as a result of condition (1). Note that the problem may be decomposed into an antenna problem with H_z^{inc} driving the slot and a problem with the transverse fields driving the slot. This is accomplished by introducing a second incident plane wave such that the total incident magnetic field becomes

$$2\underline{H}^{inc} = \underline{H}_o\, e^{i\underline{k} \cdot \underline{r}} \pm \underline{H}'_o\, e^{i\underline{k}' \cdot \underline{r}} \ ,$$

where $\underline{H}_o = H_{ox}\, \underline{e}_x + H_{oy}\, \underline{e}_y + H_{oz}\, \underline{e}_z$, $\underline{k} = k_x\, \underline{e}_x + k_y\, \underline{e}_y + k_z\, \underline{e}_z$, $\underline{H}'_o = -H_{ox}\, \underline{e}_x + H_{oy}\, \underline{e}_y + H_{oz}\, \underline{e}_z$, $\underline{k}' = -k_x\, \underline{e}_x + k_y\, \underline{e}_y + k_z\, \underline{e}_z$, $\underline{e}_j$ are unit vectors, and the plus sign yields the antenna excitation (4).

Analogous to transmission line theory, equation (12) can be written as

$$[-H_z^{>}(\rho_o^{+},z) + H_z^{>}(\rho_o^{-},z) + H_z^{sc}(z)]dz +$$

$$dI_{\rho_o} = -Y_{\rho_o} V\, dz \ , \qquad (13)$$

where $\rho_o^{\pm}$ indicates the boundary $C_{\pm}$. The quantity dI_{ρ_o} is the differential of the local

current, on the left conductor (the antenna mode consists of equal and opposite currents on the left and right conductors), in the z direction. The local current is defined by

$$I_{\rho_o} = \int_{C_{\ell cs}} \underline{H} \cdot \underline{d\ell} \ , \tag{14}$$

where the contour $C_{\ell cs}$ is over the local cross section of the left conductor, as shown in Figure 2b (note that (14) is obvious if the contour $C_{\ell cs}$ is closed by continuing it through the metal in the y direction). The local admittance per unit length Y_{ρ_o} is defined by

$$Y_{\rho_o} V = -i\omega Q_{\rho_o} + \int_{C_{\ell cs}} \sigma_g \underline{E} \cdot \underline{n} \, d\ell \ , \tag{15}$$

where Q_{ρ_o} is the electric charge per unit length on the left conductor in the local region

$$Q_{\rho_o} = \int_{C_{\ell cs}} \underline{D} \cdot \underline{n} \, d\ell \ . \tag{16}$$

Taking real and imaginary parts we may define

$$Y_{\rho_o} = G - i\omega C_{\rho_o} \ , \tag{17}$$

where C_{ρ_o} is a capacitance per unit length and G is a conductance per unit length.

Figure 3 shows the contour for the equation

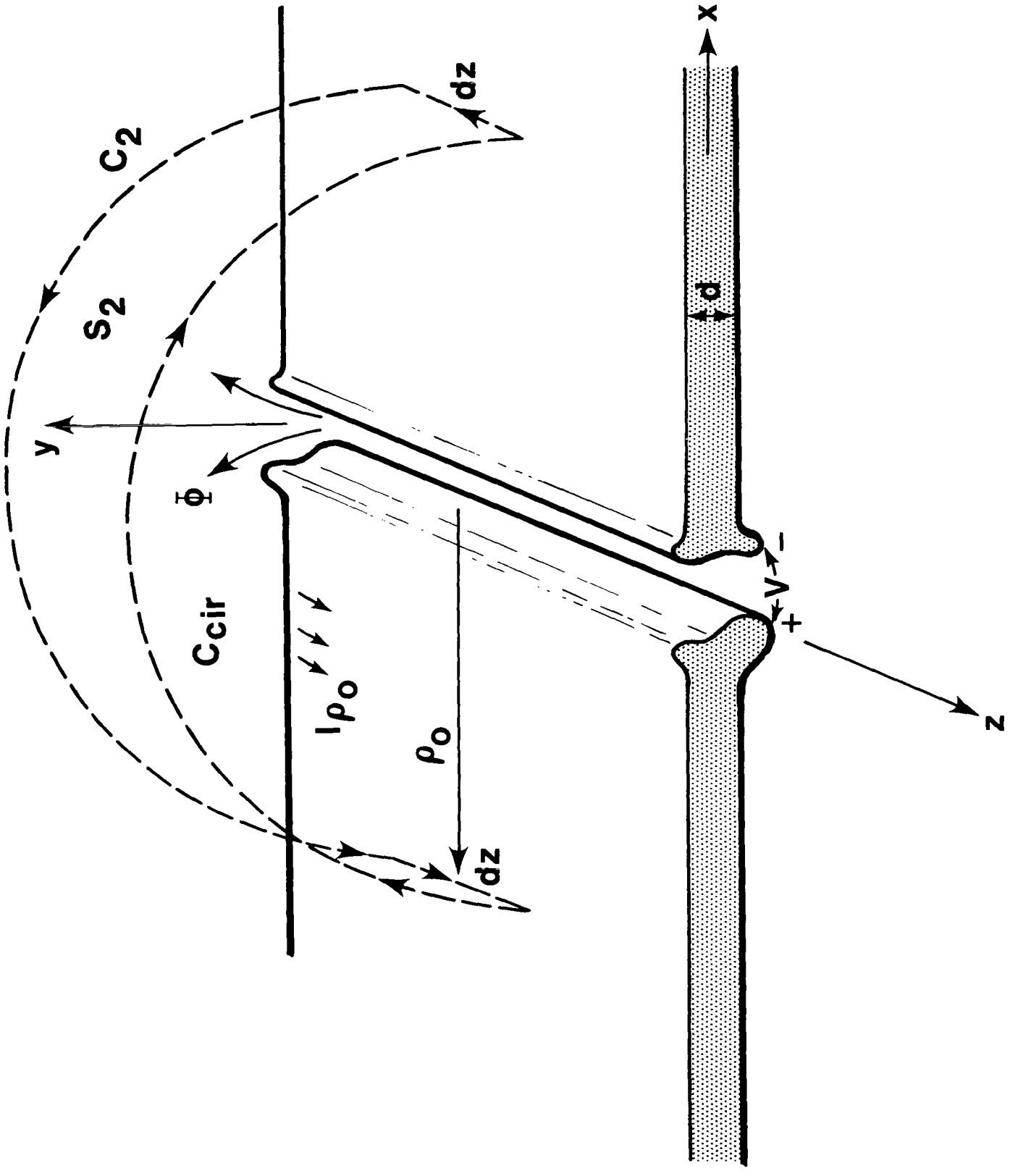

Figure 3. Contour C_2 for application of Faraday's law and Ohm's law.

$$\oint_{C_2} \underline{E} \cdot \underline{d\ell} = i\omega \int_{S_2} \underline{B} \cdot \underline{n}\, dS \ . \tag{18}$$

Analogous to standard transmission line theory, (18) becomes

$$2\, Z_S\, K_z\, dz + dV = i\omega \bar{\Phi}\, dz \ , \tag{19}$$

where [6] $Z_S = (1 - i)\, R_S$ is the surface impedance of the metal, $R_S = \frac{1}{\delta\sigma}$, the skin depth in the metal is $\delta = \sqrt{2/(\omega\mu\sigma)}$, μ is the metal magnetic permeability, σ is the metal electric conductivity, and K_z is the axial component of the effective surface current at ρ_o. Because $\rho_o >> s$ and $d >> \delta$, K_z can be found from planar considerations as $\underline{K} = \underline{n} \times \underline{H}$. The quantity dV is a differential of the voltage in the z direction, and

$$\bar{\Phi} = \int_{C_{cir}} \underline{B} \cdot \underline{n}\, d\ell \ , \tag{20}$$

where $\bar{\Phi}$ is the magnetic flux per unit length passing through the slot toward the $y > \frac{d}{2}$ half space. The contour C_{cir} is the circular contour in Figure 3 with the largest z value. If the circular contours C_{cir} in (20) and in Figure 3 are interpreted as extending several skin depths below the metal surface (with the voltage in (9) and (19) now interpreted in the same way, that is C_+ is replaced by C_{cir}), then the surface impedance term in (19) is not present because the axial electric field is zero along the contour in the metal. Alternatively, since it will be assumed that $R_S << \eta_o$, where $\eta_o = \sqrt{\mu_o \epsilon_o}$ is the free space impedance, and furthermore that $\mu\delta << \mu_o\rho_o << \mu_o\ell$, so that the surface current density at position ρ_o is small, the surface impedance term in (19) may be neglected even if the contour C_{cir} is not extended into the metal ($C_{cir} = C_+$). Equation (19) may therefore be written as

$$dV = - Z_{\rho_o} I_{\rho_o} \, dz \ , \tag{21}$$

where Z_{ρ_o} is a total series impedance defined by

$$Z_{\rho_o} I_{\rho_o} = - i\omega \Phi \ . \tag{22}$$

Note that the neglect of a nonlocal slot axial electric field $E_z^{>}(\rho_o^{\pm},z)$ and short circuit field $E_z^{sc}(z)$ relies on the assumption that the energy coupled to the nonlocal region by the axial electric field is small. This is true for small surface impedances ($R_s << \eta_o$ and $\mu\delta << \mu_o \ell$). The effect of the wall losses which is included (in the local transmission line model) is the nonnegligible power dissipation in the local region, where the surface currents are large.

Because $V_{\pm} \approx V$, from (10) and (6) we obtain

$$H_z^{>}(\rho_o^{+},z) = - H_z^{>}(\rho_o^{-},z) \ . \tag{23}$$

Substituting (23) into (13) gives

$$2H_z^{>}(\rho_o^{-},z) + H_z^{sc}(z) + \frac{d}{dz} I_{\rho_o} = Y_{\rho_o} I_m /2 \ , \tag{24}$$

where $I_m^{-} = I_m = -2V$.

Equation (21) can be written as

$$\frac{d}{dz} I_m = 2 \, Z_{\rho_o} I_{\rho_o} \ . \tag{25}$$

Substituting (25) into (24) yields the integro–differential equation

$$H_z^{>}(\rho_o^-,z) + \frac{1}{4Z_{\rho_o}}\frac{d^2}{dz^2} I_m - Y_{\rho_o} I_m /4 = - H_z^{inc} \quad , \tag{26}$$

where

$$H_z^{>}(\rho_o^-,z) = \frac{i}{\omega\mu_o}\left(\frac{d^2}{dz^2} + k^2\right) \int_{-h}^{h} \frac{e^{i\,k R_o}}{4\pi R_o} I_m(z')\, dz' \quad , \tag{27}$$

and $$R_o = \sqrt{\rho_o^2 + (z - z')^2} \, .$$

The local transmission line parameters Z_{ρ_o} and Y_{ρ_o} are evaluated by means of the local quasistatic problem. For this purpose, the boundary at ρ_o can be ignored. The only purpose of the distance ρ_o is to limit the extent of the contour $C_{\ell cs}$ so that Q_{ρ_o} and I_{ρ_o} are kept finite.

To determine C_{ρ_o} and G, a potential difference V is established between the left conductor and the right conductor by placing positive charge on the left ($x < 0$) conductor and equal and opposite charge on the right ($x > 0$) conductor. The potential V slowly oscillates at radian frequency ω. The charge Q_{ρ_o} and the conduction current through the gasket are evaluated to determine Y_{ρ_o} and thus C_{ρ_o} and G .

To determine Z_{ρ_o}, a magnetic flux through the slot Φ is established by placing z directed current on the left ($x < 0$) conductor and equal and opposite current on the right ($x > 0$)

conductor. The current I_{ρ_o} is evaluated to determine Z_{ρ_o}. The series impedance can be split into an internal part (resulting from the finite conductivity of the metal) and an external part (the series impedance when the metal conductivity is infinite). The external part is a pure inductance and therefore

$$Z_{\rho_o} = -i\omega L^{ext}_{\rho_o} + Z^{int}_{\rho_o} \quad . \tag{28}$$

The external inductance may be evaluated by taking the metal conductivity to be infinite (in which case the second term of (28) vanishes) and then solving the local magnetostatic problem for I_{ρ_o}.

When the internal impedance is negligible compared to the external impedance, the following perturbation method [7] can be used to determine $Z^{int}_{\rho_o}$.

The magnetostatic field from the infinite conductivity solution determines an electric surface current density

$$\underline{K} = \underline{n} \times \underline{H} \quad . \tag{29}$$

The complex power per unit length resulting from the finite conductivity of the conductors can be evaluated by means of

$$P_{wall} = \frac{1}{2} Z_s \int_{C_{cs}} |K_z|^2 \, d\ell \quad , \tag{30}$$

where the contour C_{cs} is over the cross section of both conductors. Note that (30) is valid,

provided that the radius of curvature of the wall, along the contour C_{cs}, is much larger than both δ and $\delta\mu/\mu^{ext}$, where μ^{ext} is the adjacent external magnetic permeability outside the metal. At sharp corners, (30) alone does not yield the correct result. Nevertheless, when the skin depth δ is very small compared to the slot dimensions and when the corner angle does not approach that of a half plane, application of (30) yields a useful estimate of the wall loss effects. The result obtained by application of (30) can be written in the form

$$P_{wall} = \frac{1}{2} D_{wall} |\underline{\Phi}|^2 \quad . \tag{31}$$

The internal impedance per unit length can be determined by setting (31) equal to

$$P_{wall} = \frac{1}{2} Z^{int}_{\rho_o} |I_{\rho_o}|^2 \quad . \tag{32}$$

Using the fact that

$$\underline{\Phi} \approx L^{ext}_{\rho_o} I_{\rho_o} \quad , \tag{33}$$

the internal impedance per unit length becomes

$$Z^{int}_{\rho_o} \approx L^{ext^2}_{\rho_o} D_{wall} \quad . \tag{34}$$

Note that, because the integral in (30) converges as the outer boundary of C_{cs} goes to infinity, D_{wall} is independent of ρ_o and thus the term introduced in (26) to account for wall loss is independent of ρ_o . Furthermore, the parameter G is independent of ρ_o because the conduction currents only exist in the region of the gasket. Although $L^{ext}_{\rho_o}$ and C_{ρ_o}

depend on ρ_o, when they are combined with the nonlocal field, which also depends on ρ_o via R_o, the dependence on ρ_o is totally eliminated. To place this fact in evidence, (26) and (27) are rewritten as

$$H_z^{>}(a,z) + \tfrac{1}{4}\left(\Delta Y_L \frac{d^2}{dz^2} I_m - \Delta Y_C I_m\right) = - H_z^{inc} \quad , \tag{35}$$

where

$$H_z^{>}(a,z) = \frac{i}{\omega\mu_o}\left(\frac{d^2}{dz^2} + k^2\right) \int_{-h}^{h} \frac{e^{i k R_a}}{4\pi R_a} I_m(z') \, dz' \quad , \tag{36}$$

$$R_a = \sqrt{(z - z')^2 + a^2} \quad ,$$

$$\Delta Y_L = \frac{1}{-i\omega L_{\rho_o}^{ext}} + \frac{Z_{\rho_o}^{int}}{\omega^2 L_{\rho_o}^{ext^2}} + \frac{1}{i\omega L_{\rho_o}^{ext^o}} \quad , \tag{37}$$

$$\Delta Y_C = G - i\omega C_{\rho_o} + i\omega C_{\rho_o}^{o} \quad , \tag{38}$$

and the quantities $L_{\rho_o}^{ext^o}$ and $C_{\rho_o}^{o}$ denote the local external inductance and capacitance per unit length without the gasket material present. These local quantities define an equivalent radius a by means of the relations

$$L_{\rho_o}^{ext^o} = \frac{\pi\mu_o}{2 \ \ell n(\rho_o/a)} \quad , \tag{39}$$

$$C_{\rho_o}^{o} = \frac{2}{\pi} \epsilon_o \, \ell n(\rho_o/a) \quad . \tag{40}$$

Note that the quantities ΔY_L and ΔY_C are independent of ρ_o .

The quantities ΔY_L and ΔY_C vanish when the gasket material is absent and the walls are perfectly conducting. Equation (35) can be integrated in this case to yield Hallén's integral equation with equivalent radius a.

When wall losses are not small, as a result of the narrowness of the slot (including sharp corner effects), the splitting

$$\frac{1}{Z_{\rho_o}} = Y^{ext}_{\rho_o} + Y^{int} \quad , \tag{41}$$

can be used. The admittance Y^{int} is independent of ρ_o, and

$$Y^{ext}_{\rho_o} = \frac{1}{-\,i\omega L^{ext}_{\rho_o}} \quad , \tag{42}$$

where this external term is determined with infinite wall conductivity. Equation (37) is now replaced by

$$\Delta Y_L = \frac{1}{-\,i\omega L^{ext}_{\rho_o}} + Y^{int} + \frac{1}{i\omega L^{ext^o}_{\rho_o}} \quad . \tag{43}$$

Note that, particularly in the case of large losses, the uniformity of the local transverse voltage over the cross section must be confirmed. Previously [1] Faraday's law (18) was used to estimate the odd component of the voltage when the slot was symmetric in the depth (y direction) and was driven asymmetrically (one half (4) was assumed incident on

both sides of the slot). The general slot considered in the present case is not symmetric in the depth. Nevertheless, application of Faraday's law in the same manner results in a useful estimate of the nonuniformity of the voltage in the depth. The axial magnetic field in the slot is taken to be approximately (4). Reference to Figure 4 shows that the change in voltage from one side of the slot to the other is approximately

$$2\Delta V \approx -[(s_- + s_+)Z_s - i\omega(\mu_g A_g + \mu_o A_o)]H_z^{inc}(z) \quad , \tag{44}$$

where distances s_- and s_+ are along the left and right metal surfaces, areas A_g and A_o are the enclosed areas of the gasket and free space regions, and μ_g is the gasket magnetic permeability. Approximate uniformity of the voltage is indicated when $V >> \Delta V$.

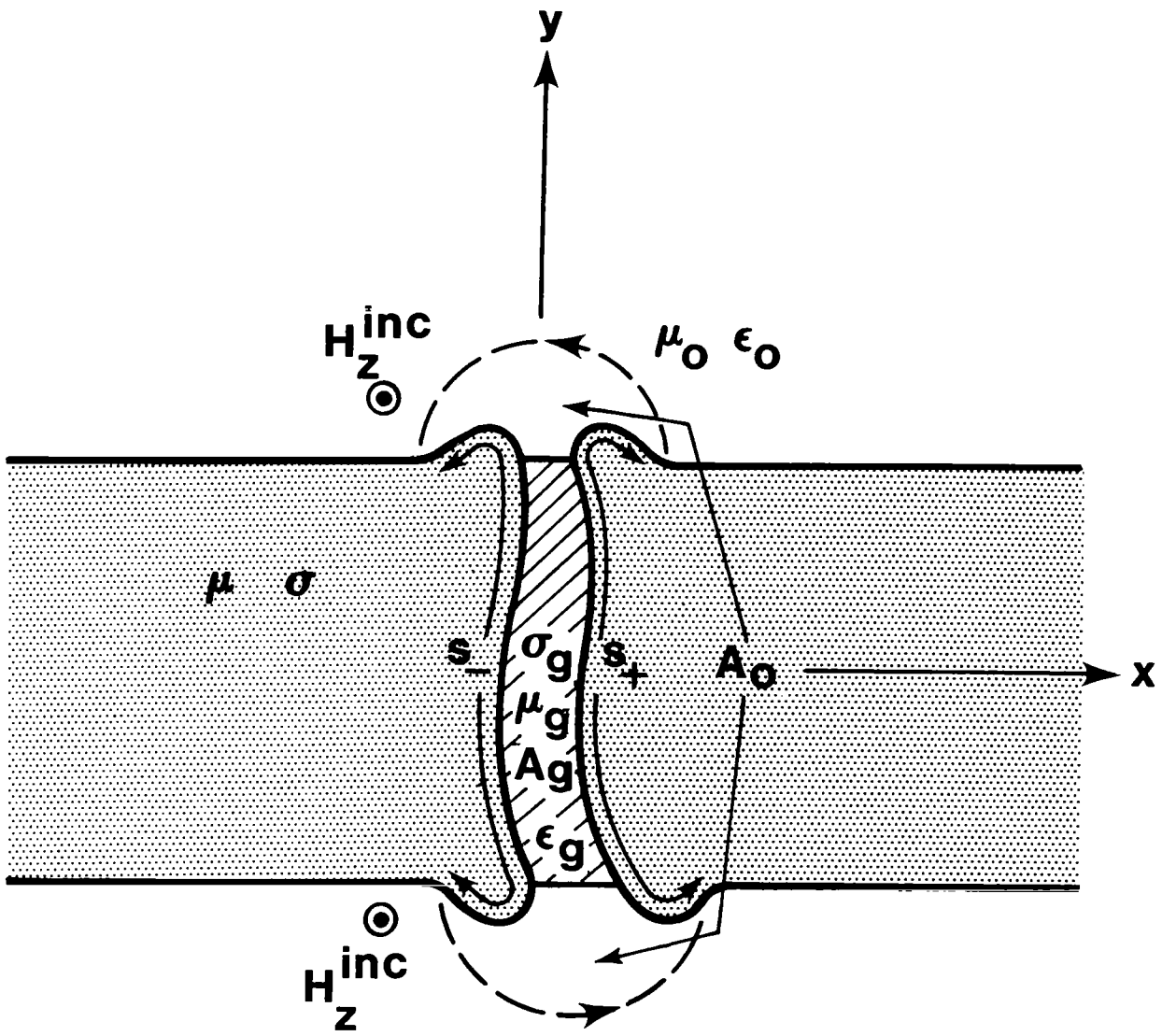

Figure 4. Slot aperture geometry with asymmetric excitation (H_z^{inc} is even in the depth). The change in voltage $2\Delta V$ equals the line integral of $\underline{E}$ over the two circular dashed contours.

III. EXAMPLES

Five examples involving a rectangular slot aperture of width w, depth d, and length ℓ (ℓ, λ >> w, d), shown in Figure 5, are now considered. The following notation is used:

int = internal to the metal walls of the conducting plane,

ext = external to the metal walls of the conducting plane,

intr = interior to the rectangular slot ($-\frac{d}{2} < y < \frac{d}{2}, -\frac{w}{2} < x < \frac{w}{2}$),

extr = exterior to the rectangular slot ($y \gtrless \pm \frac{d}{2}$).

1. Lossless without gaskets

The equivalent radius can be obtained from conformal mapping [1] as

$$a = -C_1 \sqrt{p} \ , \tag{45}$$

where p is obtained by solving the transcendental equation

$$2\frac{d}{w} = -\frac{2E(p') - (1 + p^2)K(p')}{2E(p) - (1 - p^2)K(p)} \ , \tag{46}$$

where K(p) and E(p) are the complete elliptic integrals

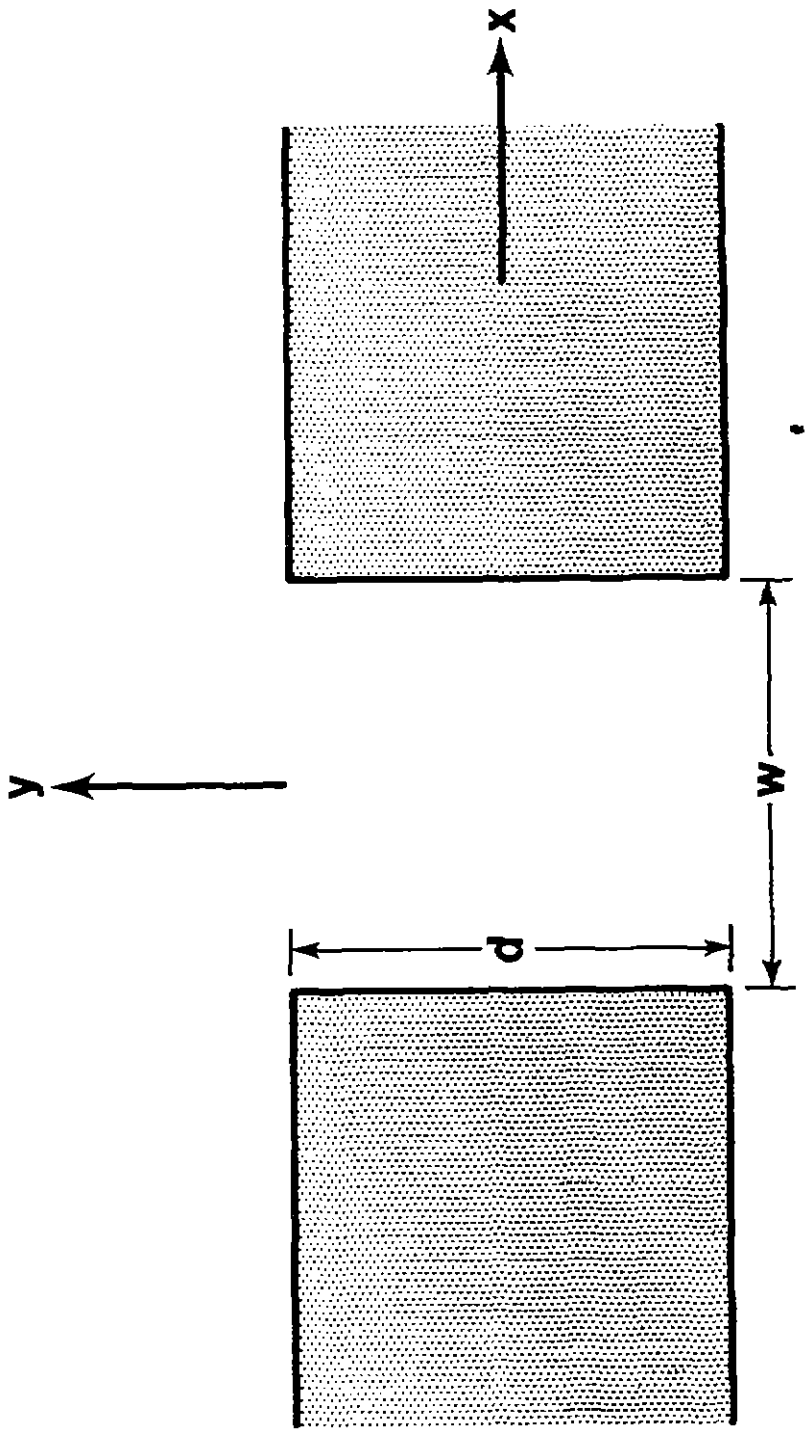

Figure 5. Rectangular slot aperture geometry.

$$K(p) = \int_0^{\pi/2} \frac{d\theta}{\sqrt{1 - p^2 \sin^2\theta}} , \tag{47}$$

$$E(p) = \int_0^{\pi/2} \sqrt{1 - p^2 \sin^2\theta}\, d\theta , \tag{48}$$

and

$$p' = \sqrt{1 - p^2} . \tag{49}$$

The quantity C_1 can be found from

$$\frac{w}{2C_1} = (1 - p^2)K(p) - 2E(p) . \tag{50}$$

Asymptotic solutions can easily be found [1] as

$$a \to \frac{w}{4} , \frac{d}{w} \to 0 , \tag{51}$$

$$a \sim \frac{2}{\pi} w / e^{\left(1 + \frac{\pi d}{2w}\right)} , \frac{d}{w} >> 1 . \tag{52}$$

A useful approximation can be obtained [1] by approximating the local field distribution as the thin slot ($d = 0$) field distribution exterior to the slot and a uniform field distribution interior to the slot. The approximate equivalent radius is

$$a \approx \frac{w}{4} e^{-\frac{\pi d}{2w}} . \tag{53}$$

The antenna fatness parameter defined by

$$\Omega = 2\,\ell n(2h/a) \quad , \tag{54}$$

where $2h = \ell$, has the particularly simple form

$$\Omega \approx 2\,\ell n(4\ell/w) + \pi\frac{d}{w} \quad , \tag{55}$$

when the approximation (53) is used.

2. Low loss wall material without gasket

The external inductive reactance will dominate the internal wall impedance provided

$$\mu_o w,\ \mu_o d >> \mu\delta \quad . \tag{56}$$

The equivalent radius is again (45). The lossless transverse magnetostatic problem can be solved by conformal mapping to yield the axial current distribution by means of (29). Equation (30) then gives the complex power per unit length. Referring to (31), this can be written as [8]

$$D_{wall} = D^{extr} + D^{intr} \quad , \tag{57}$$

where

$$D^{extr} = \frac{4Z_s K(p)}{-\,C_1 \mu_o^2 \pi^2} \quad , \tag{58}$$

$$D^{intr} = \frac{2Z_s K(p')}{-C_1 \mu_o^2 \pi^2} \quad , \tag{59}$$

where D^{extr} arises from the exterior axial slot current ($y = \pm \frac{d}{2}$, $x \gtrless \pm \frac{w}{2}$) and D^{intr} arises from the interior axial slot current ($x = \pm \frac{w}{2}$, $-\frac{d}{2} < y < \frac{d}{2}$). Note that for very thick slots ($d/w >> 1$) [8] these can be expanded as

$$D^{extr} \sim \frac{2Z_s}{w\mu_o^2} \quad , \tag{60}$$

$$D^{intr} \sim \frac{2}{\pi} D^{extr} + \frac{2Z_s}{d}/(\mu_o \frac{w}{d})^2 \quad , \tag{61}$$

where the dominant second term in (61) arises from a uniform interior field.

Figures 6 through 8 give normalized center voltage magnitude and radiated power (equal to approximately twice the transmitted power) for the perfectly conducting case and for aluminum, titanium, and stainless steel walls. The equivalent radius (45), along with equations (57), (58), (59), (34), and (37) were used in (35) and (36) to generate these figures. The Galerkin method with piecewise sinusoidal basis functions [1]

$$I_m(z) = \sum_{n=-N}^{N} I_{mn} F_n(z) \quad , \tag{62}$$

where

$$F_n(z) = \frac{\sin(kz - kz_{n-1})}{\sin(kz_n - kz_{n-1})} \quad , z_{n-1} \leq z < z_n \, ,$$

$$= \frac{\sin(kz_{n+1} - kz)}{\sin(kz_{n+1} - kz_n)} \quad , z_n \leq z < z_{n+1} \, ,$$

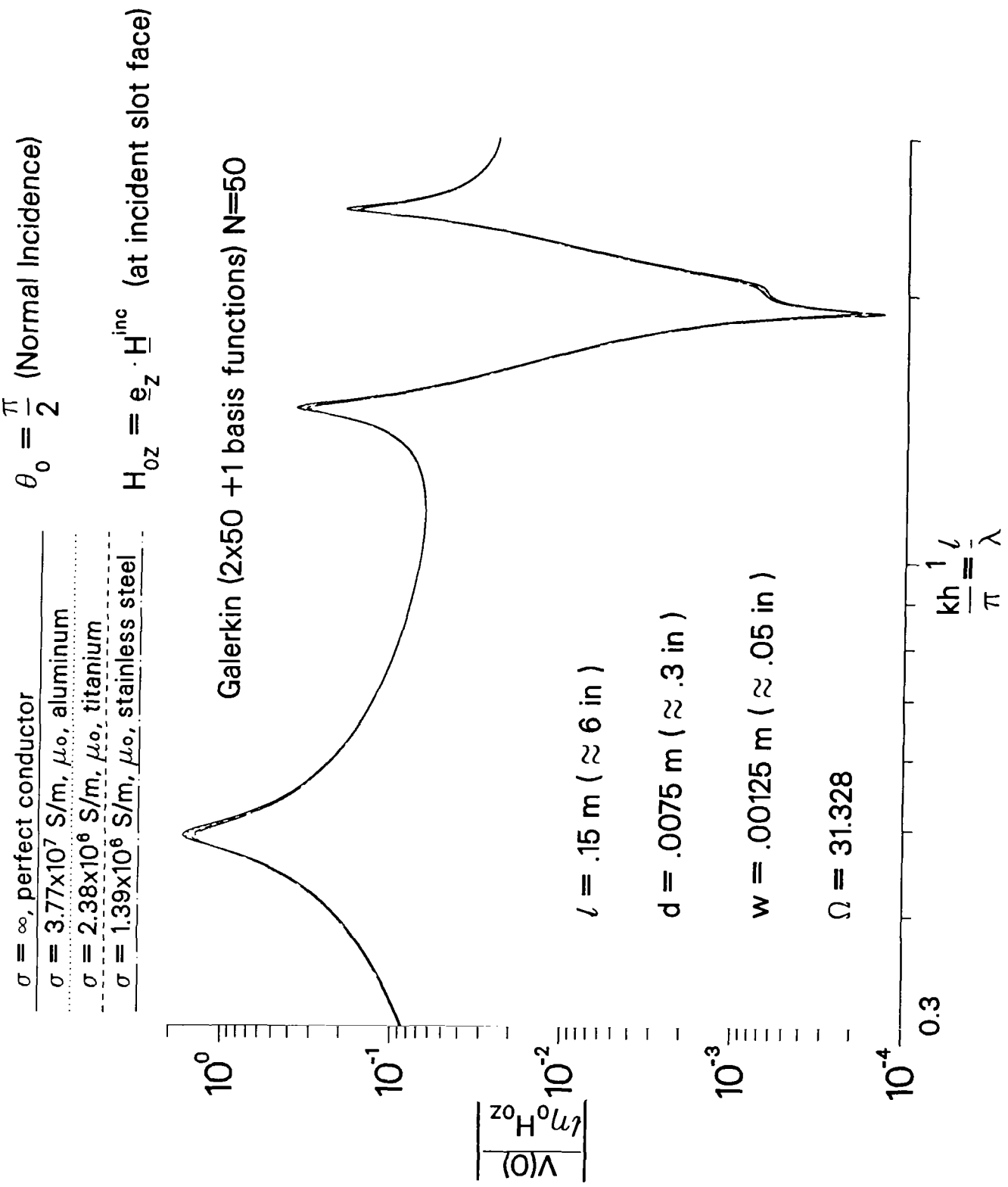

Figure 6. Wall loss effects are illustrated for a rectangular slot aperture approximately 6 inches in length, 0.3 inches in depth, and 0.05 inches in width. (a) Normalized center voltage magnitude.

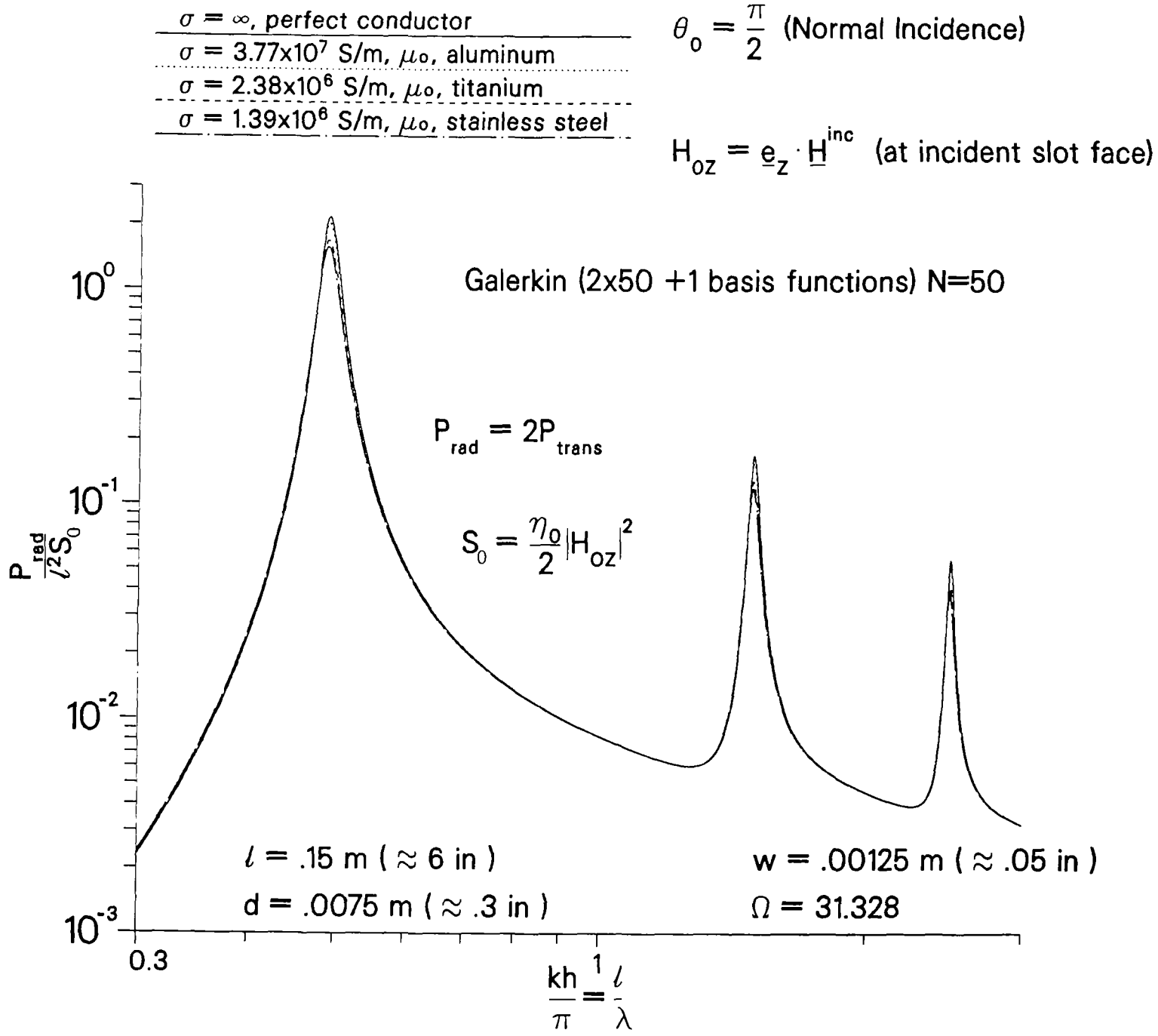

(b) Normalized radiated power.

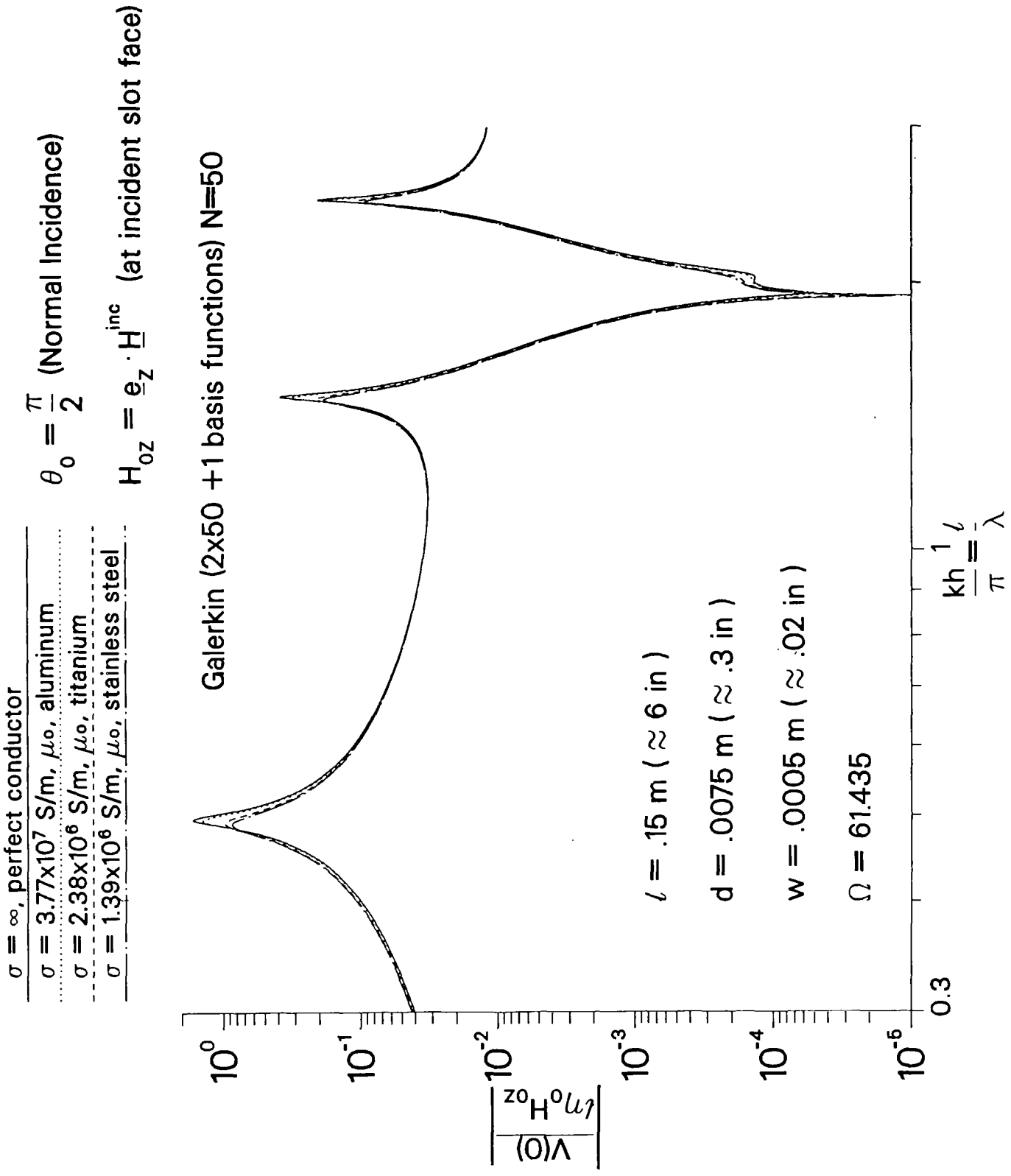

Figure 7. Wall loss effects are illustrated for a rectangular slot aperture approximately 6 inches in length, 0.3 inches in depth, and 0.02 inches in width. (a) Normalized center voltage magnitude.

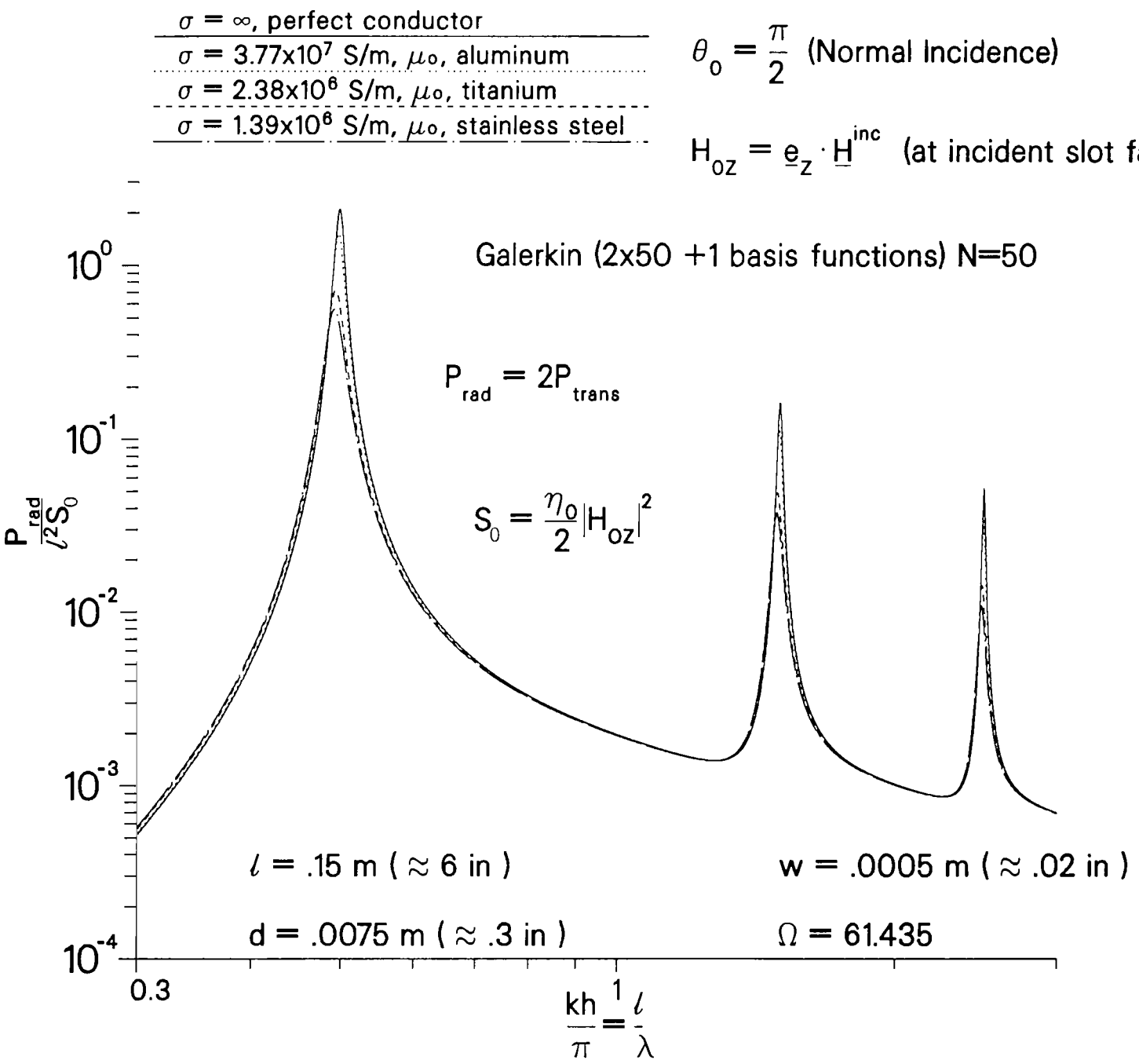

(b) Normalized radiated power.

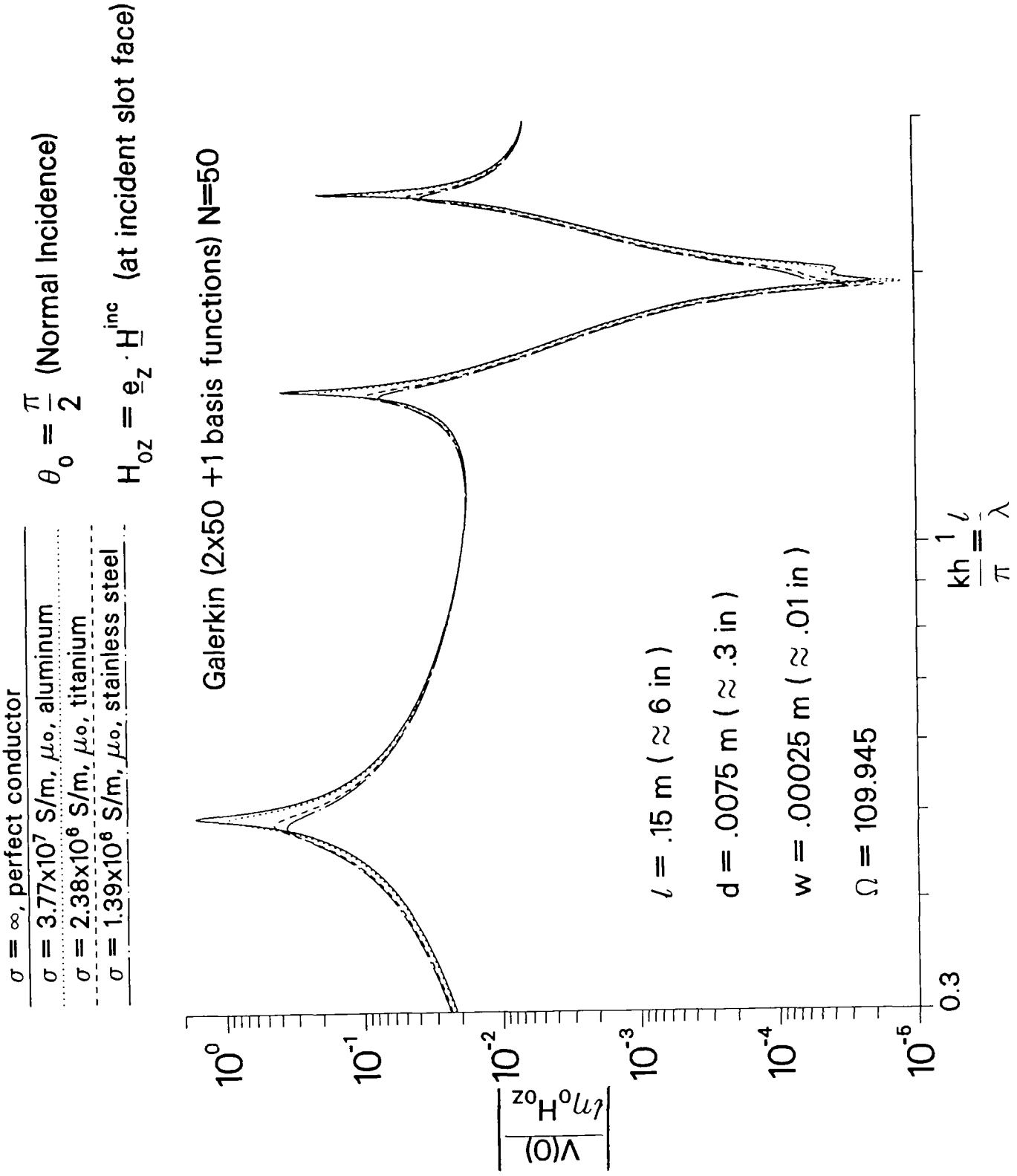

Figure 8. Wall loss effects are illustrated for a rectangular slot aperture approximately 6 inches in length, 0.3 inches in depth, and 0.01 inches in width. (a) Normalized center voltage magnitude.

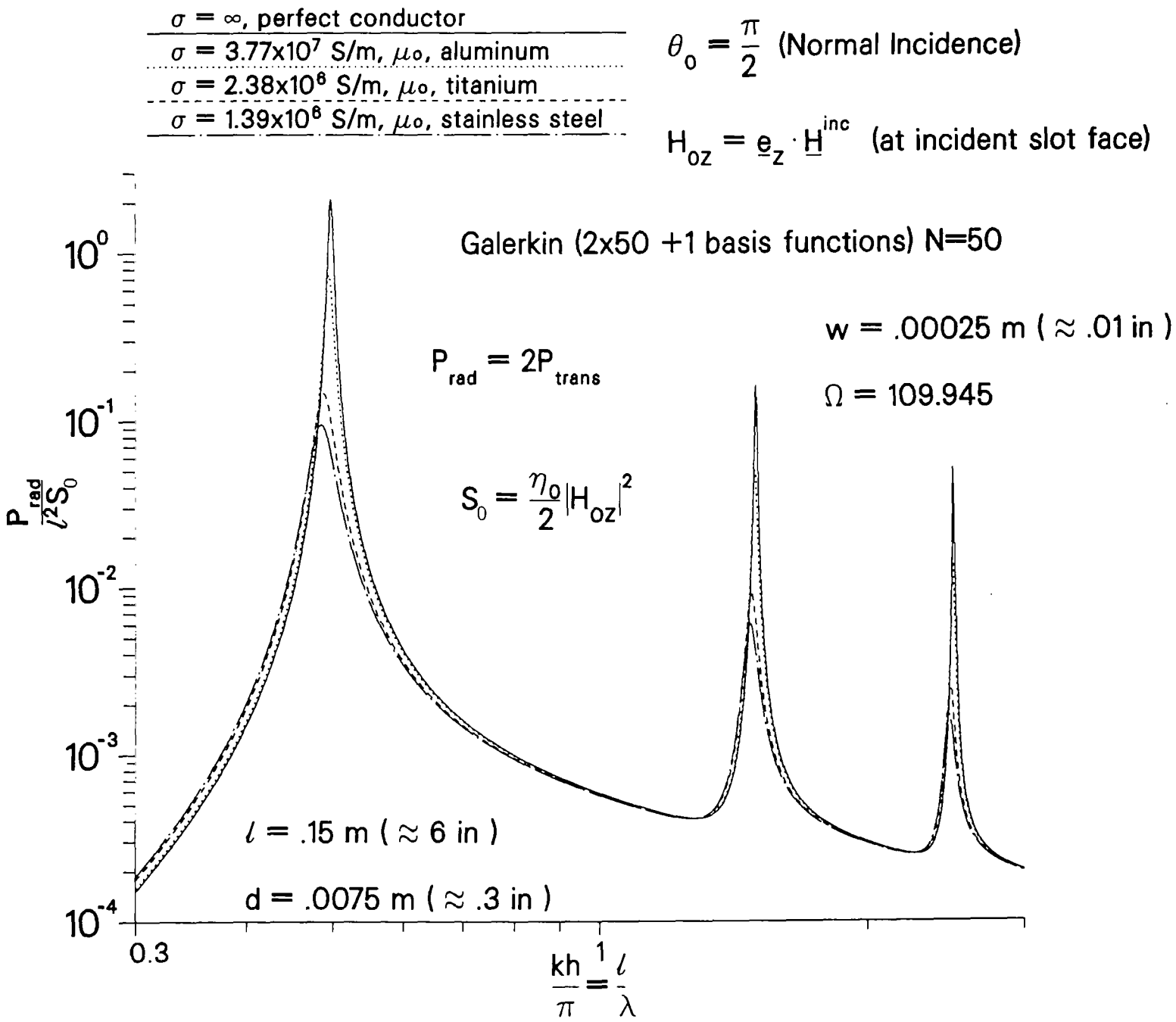

(b) Normalized radiated power.

$= 0$, otherwise ,

was used to solve the integro–differential equation (35). Uniform spacing $z_n = n\Delta$, where $\Delta = h/(N+1)$, was chosen.

3. Very thick rectangular slot (d >> w) with large losses ($\delta\mu$ same order or bigger than $w\mu_o$, $\mu_o d >> \mu\delta$) without gasket

The approximate equivalent radius (53) is used in this example.

Rigorous evaluation of the losses and Y^{int} now poses a difficult problem in general. The exterior axial current distribution near the slot and the interior current distribution near the slot edges are altered (relative to the perfectly conducting distribution) because of the nonzero surface impedance. However, because the slot is very thick, the dominant losses arise from a nearly uniform interior field. This statement is true as long as the slot interior walls carry most of the local axial current.

Figure 9 shows the approximate local transmission line model for the very thick slot. In accord with use of the approximate equivalent radius (53), the inductance and capacitance per unit length may be approximated by those corresponding to a thin slot exterior field and a uniform interior field. The thin slot exterior field results in an inductance per unit length

$$L^{extr}_{\rho_o} \approx \frac{\pi\mu_o}{2\ \ell n\left[\frac{\rho_o}{w/4}\right]} \ . \qquad (63)$$

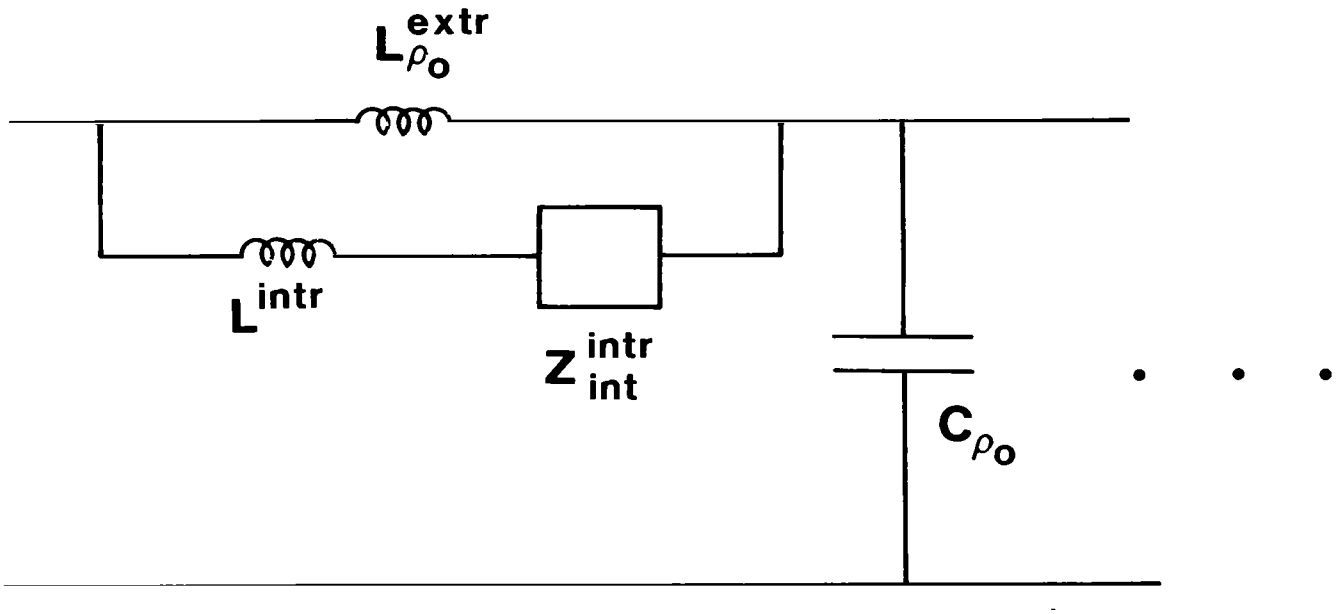

Figure 9. Local circuit model of very thick rectangular slot aperture with large wall losses.

The uniform interior field results in an external inductance per unit length

$$L^{intr} \approx \mu_o \frac{w}{d} \ , \tag{64}$$

and internal impedance per unit length

$$Z_{int}^{intr} \approx \frac{2Z_s}{d} \ , \tag{65}$$

where the factor of 2 in (65) arises from the fact that there are two walls. The capacitance per unit length is

$$C_{\rho_o} \approx \frac{2}{\pi} \epsilon_o \, \ell n\left[\frac{\rho_o}{w/4}\right] + \epsilon_o \frac{d}{w} \ , \tag{66}$$

where the first term corresponds to the thin slot exterior field and the second term corresponds to a uniform interior field.

The wall losses exterior to the slot have been ignored in the preceding circuit model. As the quantity $\mu\delta$ becomes nonnegligible compared to $\mu_o w$, the local exterior axial current density becomes more uniform than that predicted by the perfectly conducting magnetostatic result. This action tends to decrease (relative to the perfectly conducting axial current distribution) the power dissipation due to the exterior wall materials but increase the exterior external inductance. Therefore, by imposing the condition

$$|Z_{int}^{intr} - i\omega L^{intr}| << \omega L_{\rho_o}^{extr} \ , \tag{67}$$

or, alternatively, because $\Omega^{extr} > 2 \, \ell n(4\rho_o/w)$,

$$\sqrt{\mu^2\delta^2 + (\mu\delta + \mu_o w)^2} << \mu_o d \frac{\pi}{\Omega^{extr}} , \tag{68}$$

where $$\Omega^{extr} = 2\,\ell n(4\ell/w) , \tag{69}$$

most of the local axial current is carried by the slot interior.

A further required condition to ensure validity of the interior part of the circuit model (typically much less stringent than the conditions required to neglect the variation of the voltage with depth) is $\frac{\omega\epsilon_o}{w} << \frac{\sigma}{\delta}$. The transverse voltage appears across the capacitance of the gap (or gasket with $\epsilon_o \to \epsilon_g$) rather than in the walls when this condition is met.

The inverse of the series impedance per unit length can be found from (41) and (42), where

$$\frac{1}{L^{ext}_{\rho_o}} = \frac{1}{L^{extr}_{\rho_o}} + \frac{1}{L^{intr}} , \tag{70}$$

gives the external inductance per unit length and

$$Y^{int} \approx \frac{Z^{intr}_{int}}{i\omega L^{intr}(Z^{intr}_{int} - i\omega L^{intr})} , \tag{71}$$

or

$$Y^{int} \approx \frac{2Z_s/d}{i\omega\mu_o\frac{w}{d}\left[2Z_s/d - i\omega\mu_o\frac{w}{d}\right]} . \tag{72}$$

Equation (72) can now be used in (43) along with the approximate equivalent radius (53) to include the external inductance per unit length (70) and capacitance per unit length(66).

Figures 10 through 12 give normalized center voltage magnitude and radiated power for the perfectly conducting case and for aluminum, titanium, and stainless steel walls.

The rectangular slot aperture has a plane of symmetry at y = 0. Thus application of Faraday's law (18) to the slot interior, see Figure 13 (the axial magnetic field intensity in the odd problem is approximately (4)), yields the odd voltage

$$V_{odd} \approx (2Z_s - i\omega\mu_g w) y \, H_z^{inc}(z) \quad , -\frac{d}{2} \leq y \leq \frac{d}{2} . \tag{73}$$

The gasket magnetic permeability μ_g is μ_o in this case. The addition of V_{odd} to V when y $= -\frac{d}{2}$ yields an approximation to the voltage at the illuminated slot face. Alternatively, this sum, when $y = \frac{d}{2}$, yields an approximation to the voltage at the unilluminated slot face. Figures 14 and 15 show the even voltage magnitude and the corrections resulting from addition of (73) for the geometry of Figures 11 and 12, respectively. Notice the expected large correction at the voltage minimum near kh = 2π. The correction also has an effect at the upper limit of the abscissa for which kd approaches unity.

Figures 16 and 17 give examples with wall materials having conductivities representative of conductive composites. Figures 18 and 19 show the effect of the odd problem correction.

4. Lossy gasket without wall loss

The geometry of the slot with gasket is shown in Figure 20. The approximate equivalent

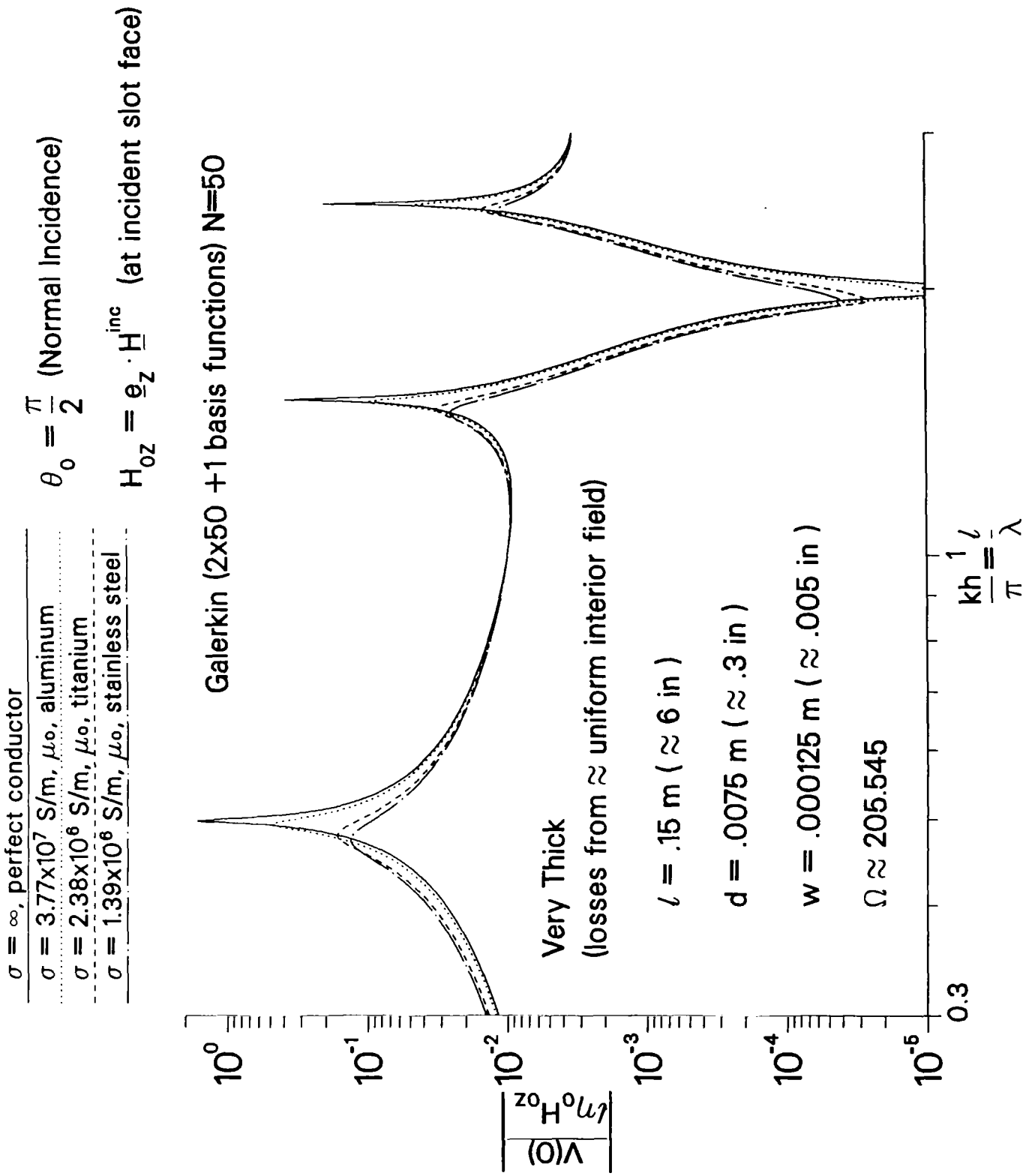

Figure 10. Wall loss effects are illustrated for a rectangular slot aperture approximately 6 inches in length, 0.3 inches in depth, and 0.005 inches in width. (a) Normalized center voltage magnitude.

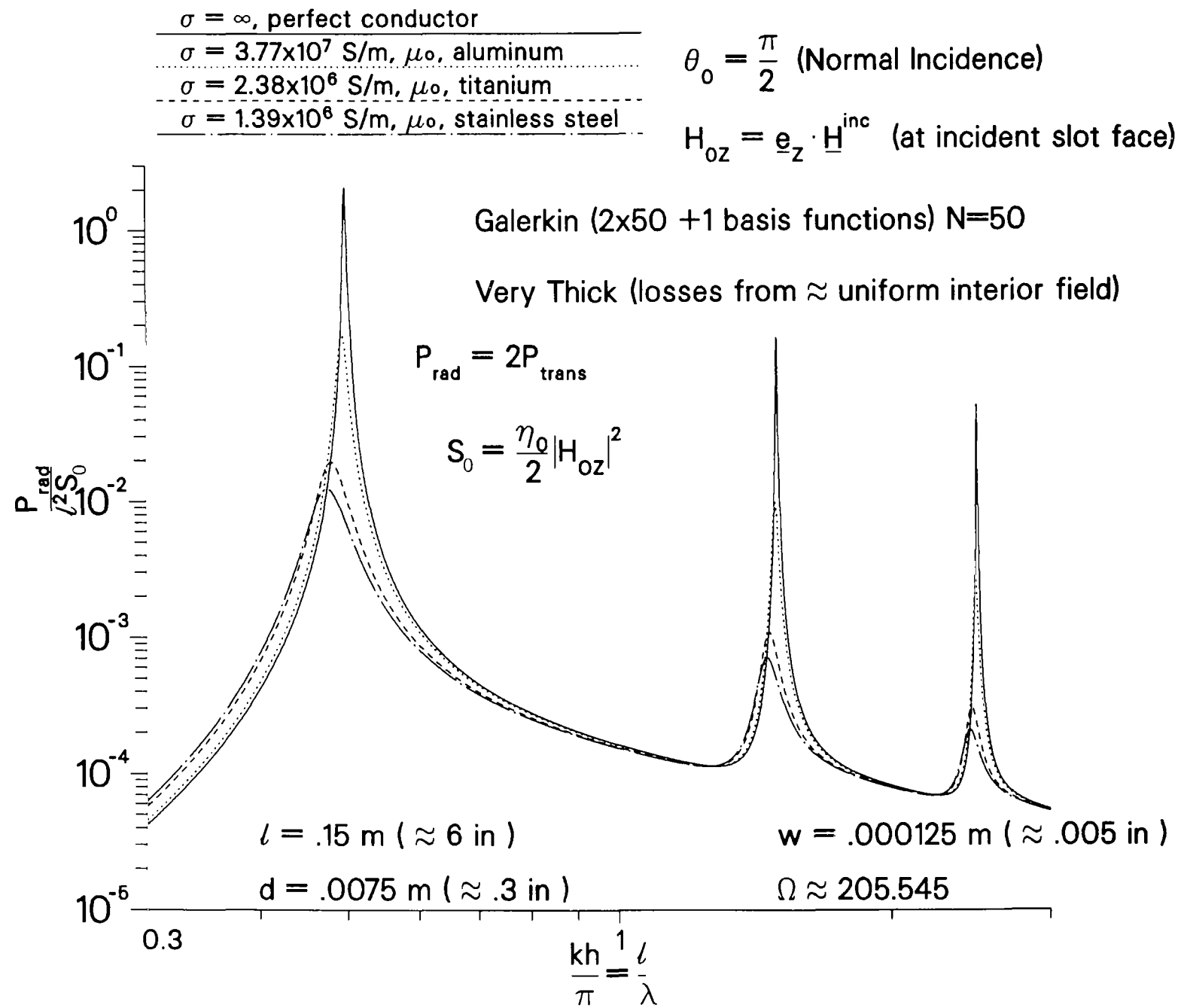

(b) Normalized radiated power.

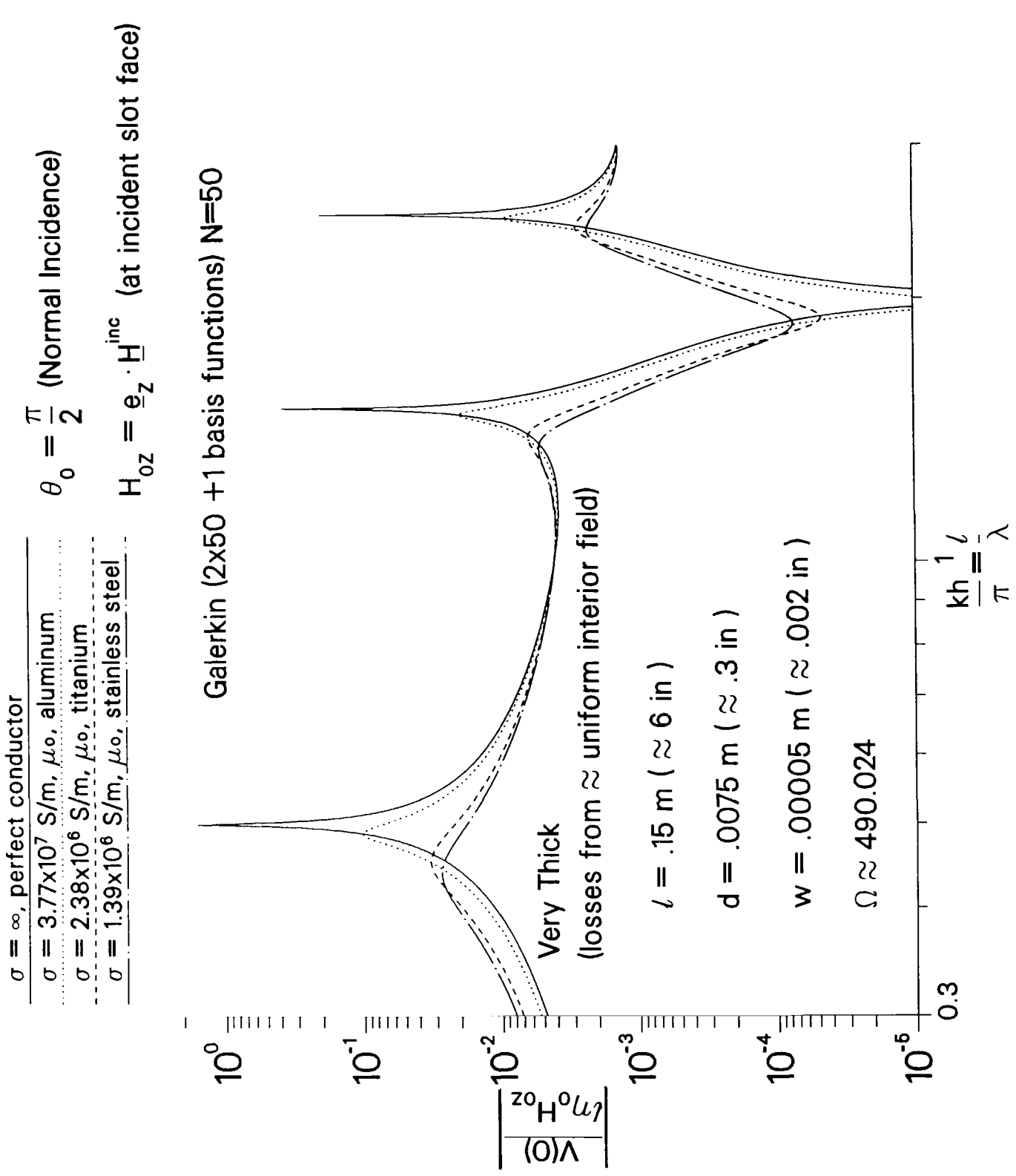

Figure 11. Wall loss effects are illustrated for a rectangular slot aperture approximately 6 inches in length, 0.3 inches in depth, and 0.002 inches in width. (a) Normalized center voltage magnitude.

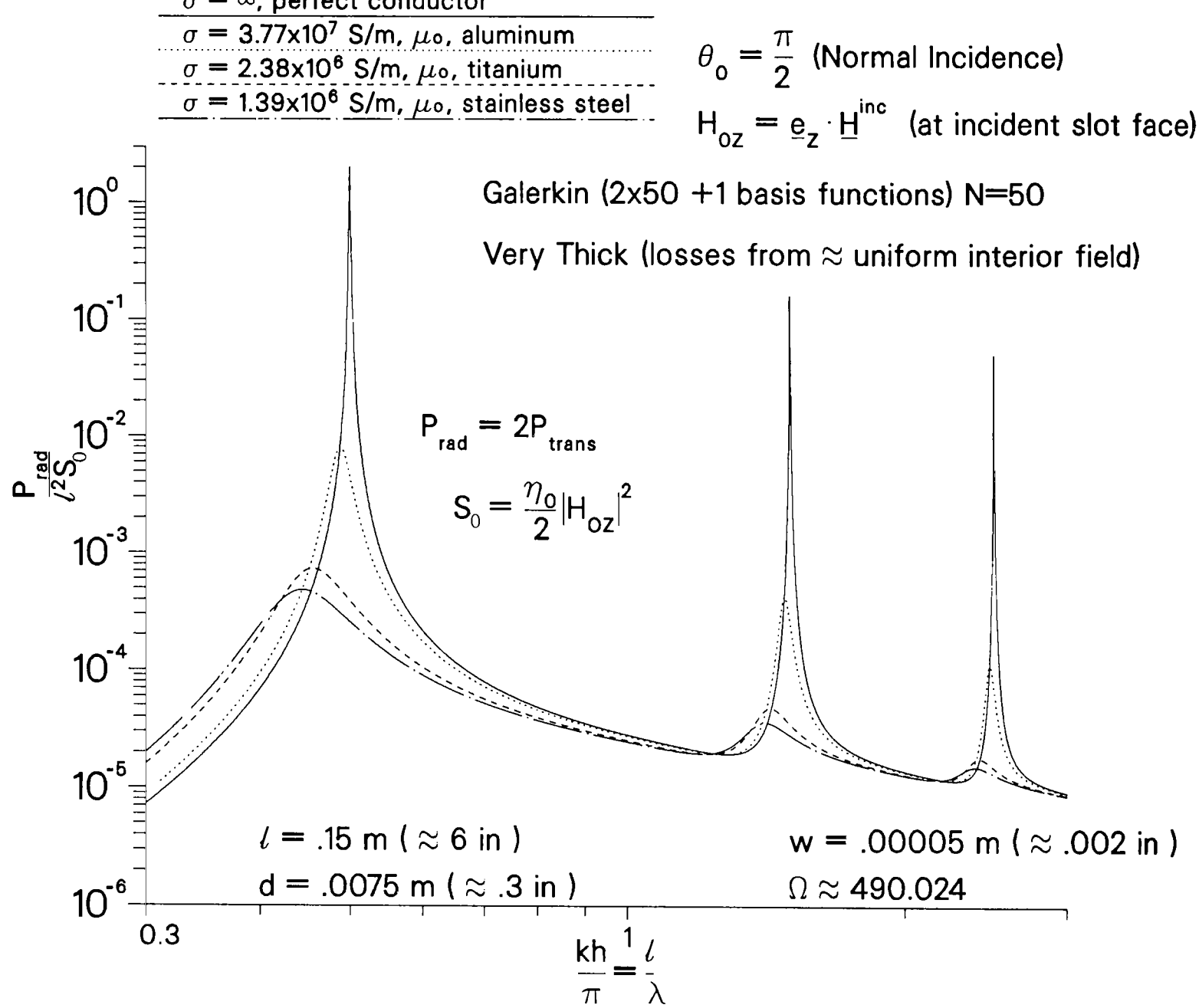

(b) Normalized radiated power.

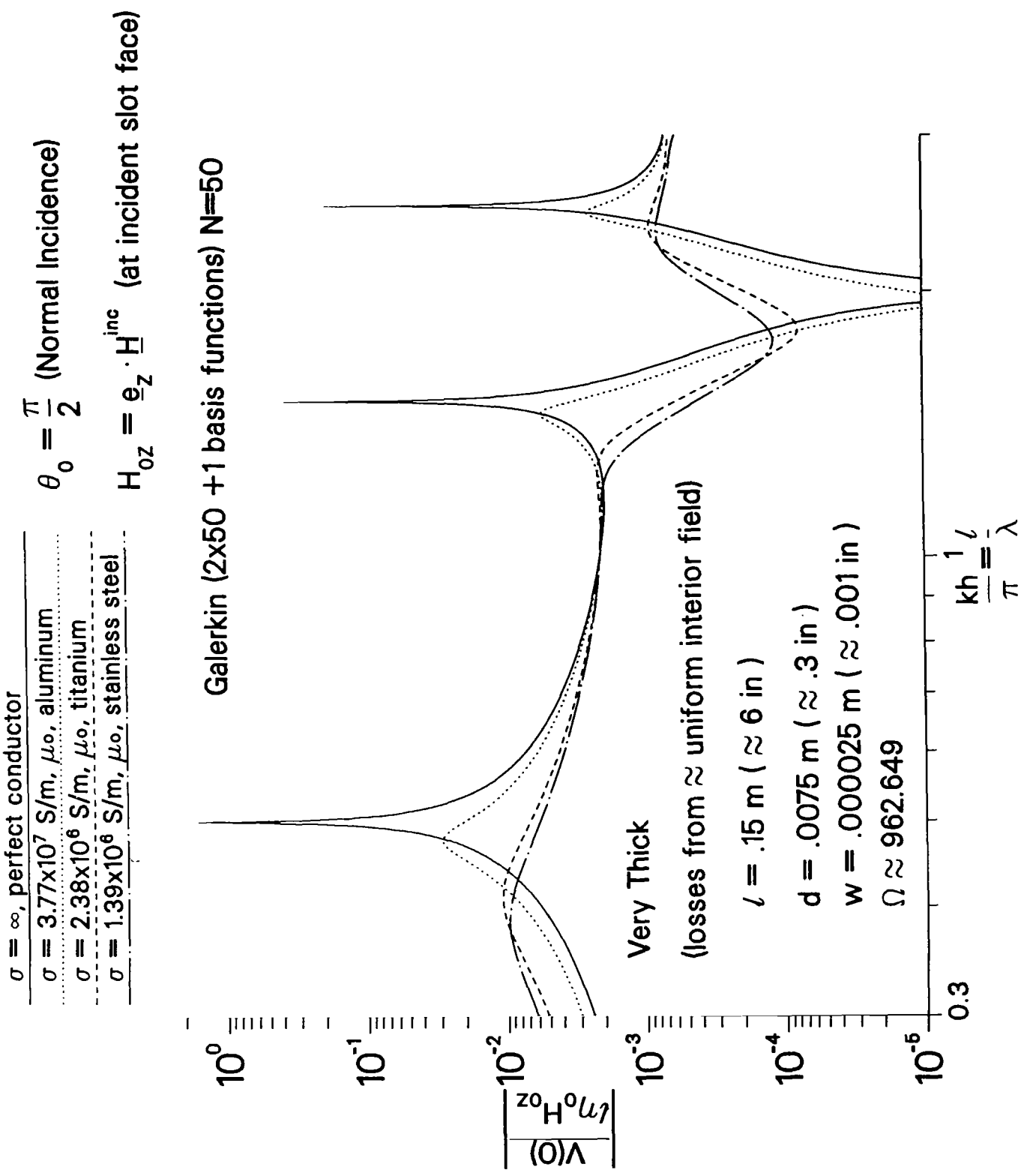

Figure 12. Wall loss effects are illustrated for a rectangular slot aperture approximately 6 inches in length, 0.3 inches in depth, and 0.001 inches in width. (a) Normalized center voltage magnitude.

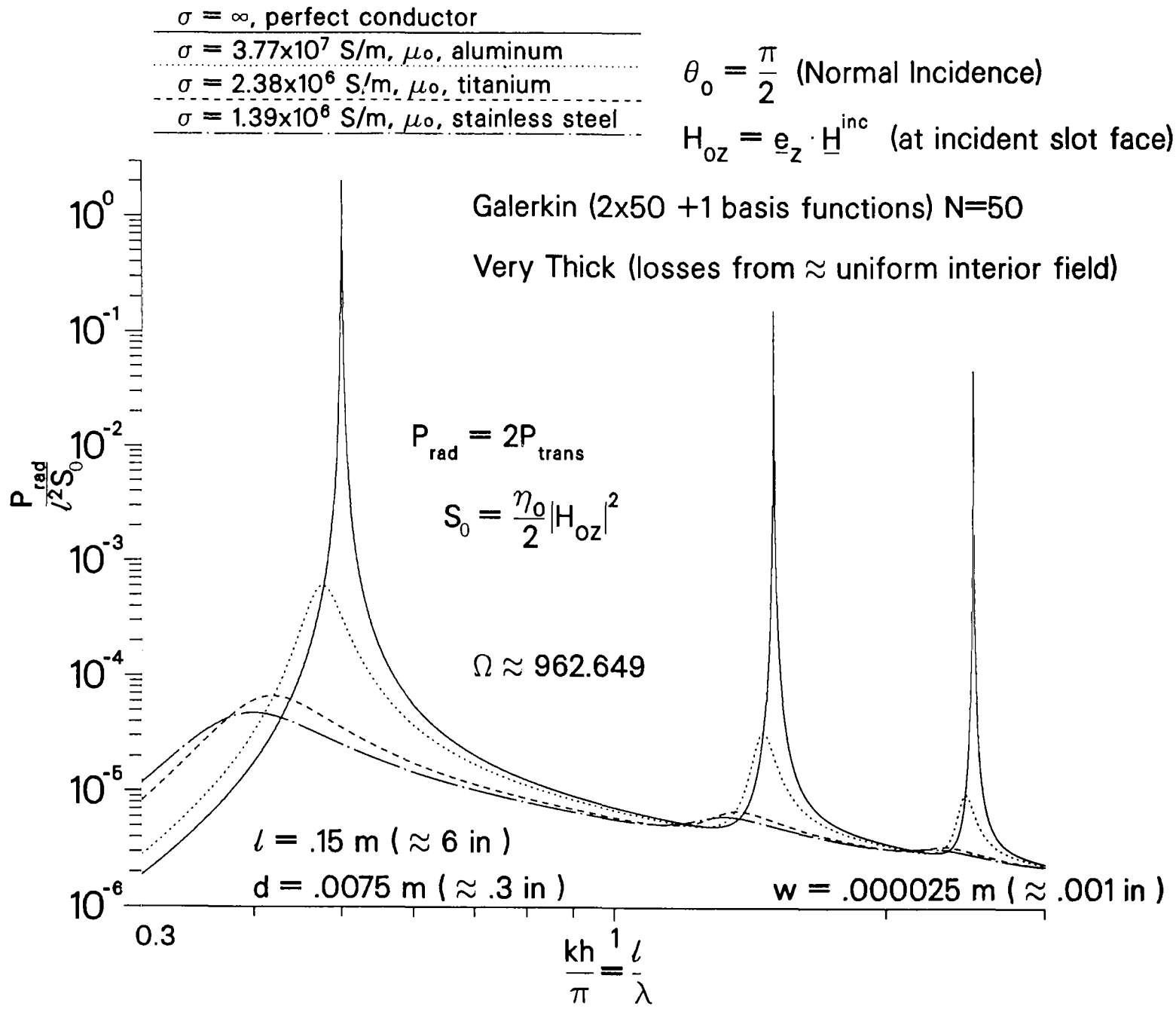

(b) Normalized radiated power.

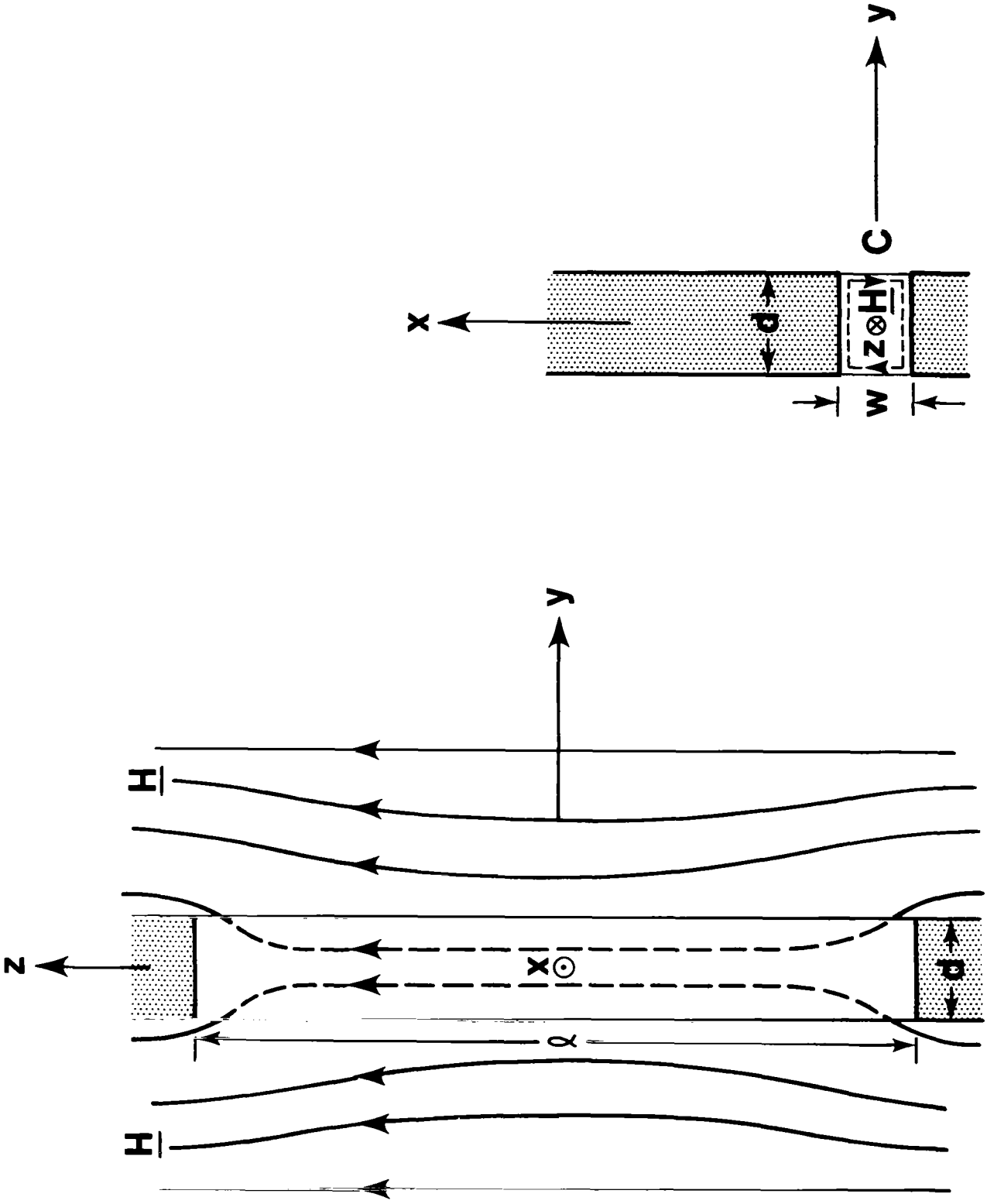

Figure 13. Rectangular slot odd problem. (a) Magnetic field lines. (b) Faraday's law contour.

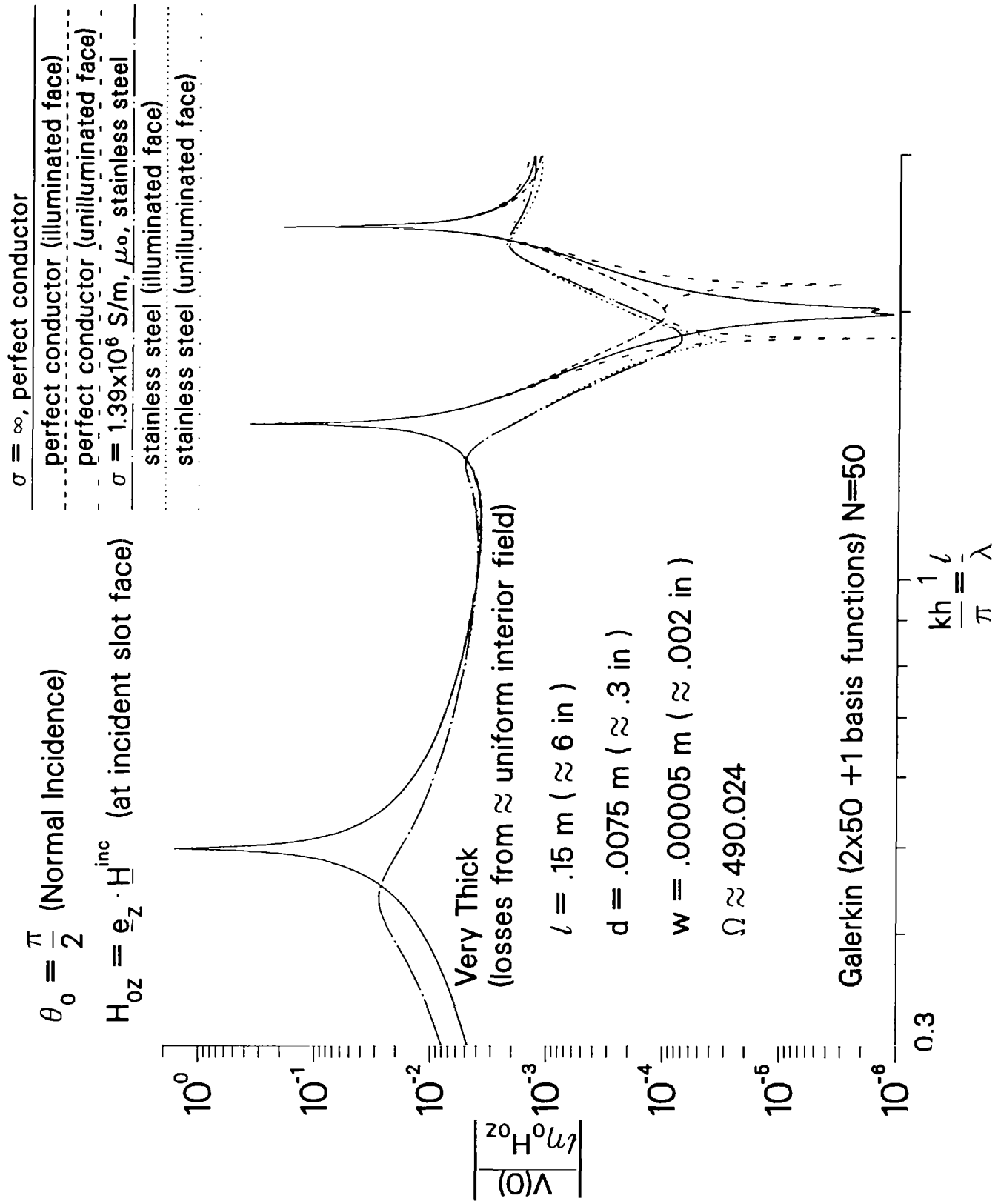

Figure 14. Normalized center voltage magnitude for the geometry of Figure 11. Also shown are the corrections obtained by addition of the odd solution.

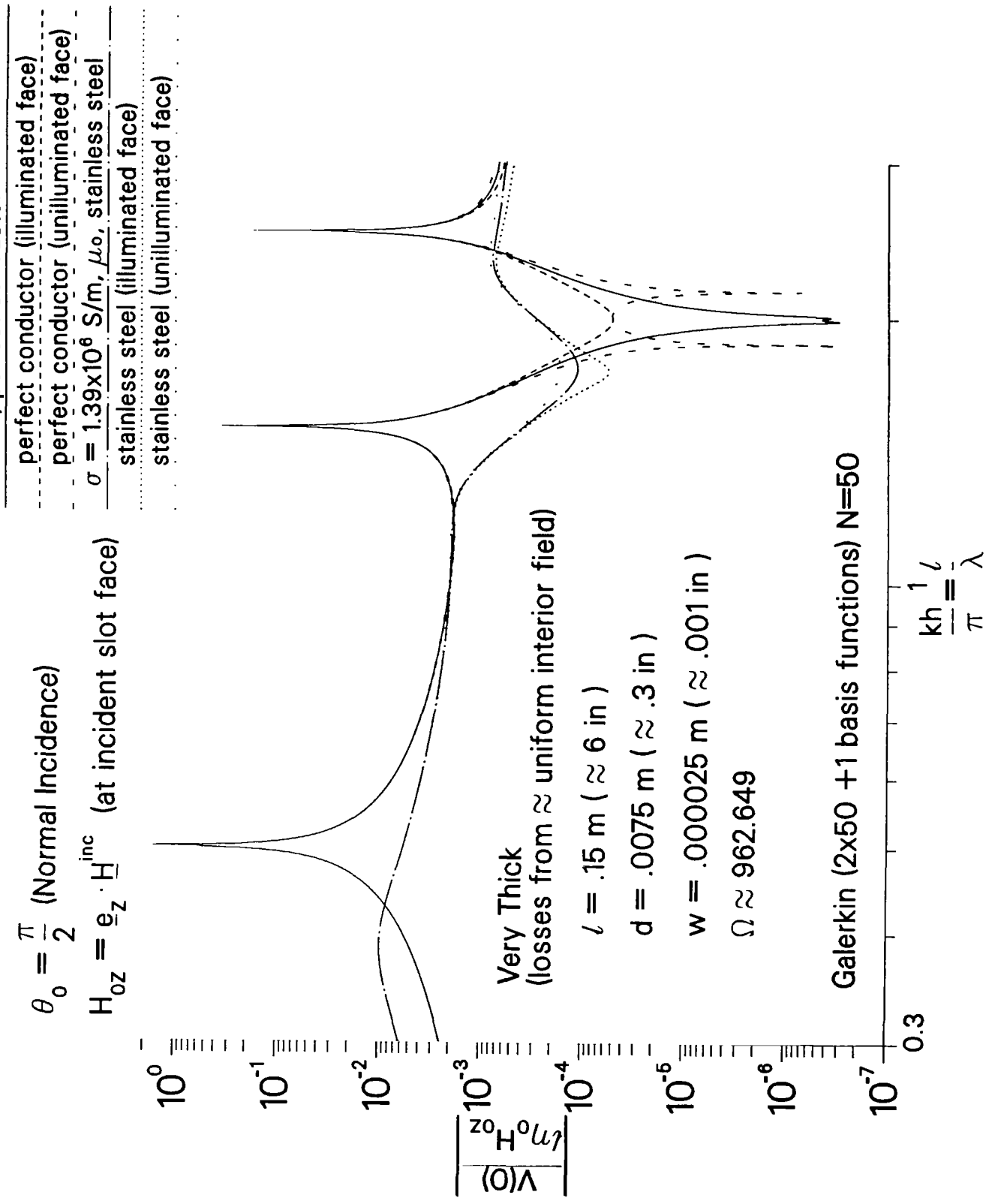

Figure 15. Normalized center voltage magnitude for the geometry of Figure 12. Also shown are the corrections obtained by addition of the odd solution.

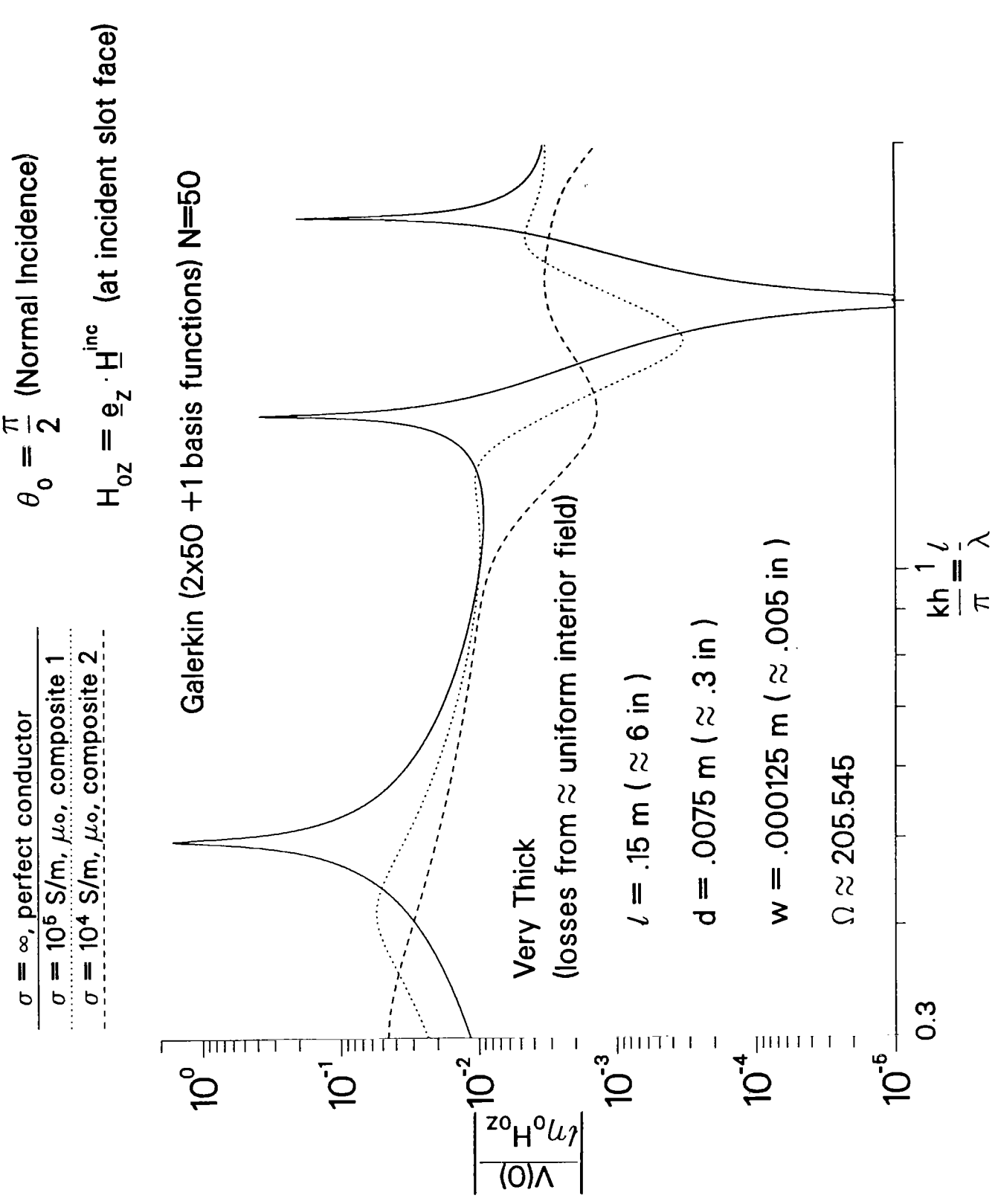

Figure 16. Conductive composite wall material effects are illustrated for a rectangular slot aperture approximately 6 inches in length, 0.3 inches in depth, and 0.005 inches in width. (a) Normalized center voltage magnitude.

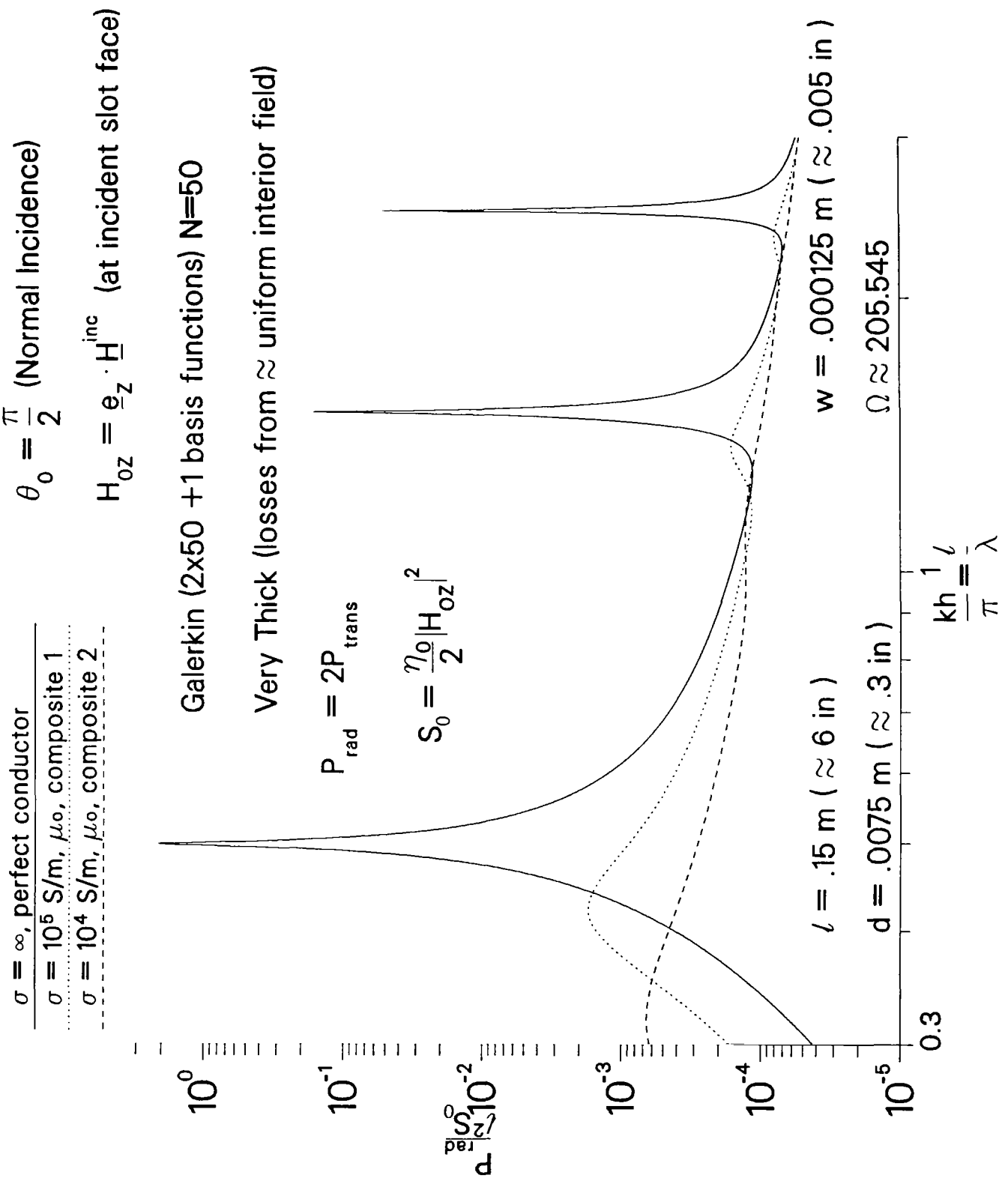

(b) Normalized radiated power.

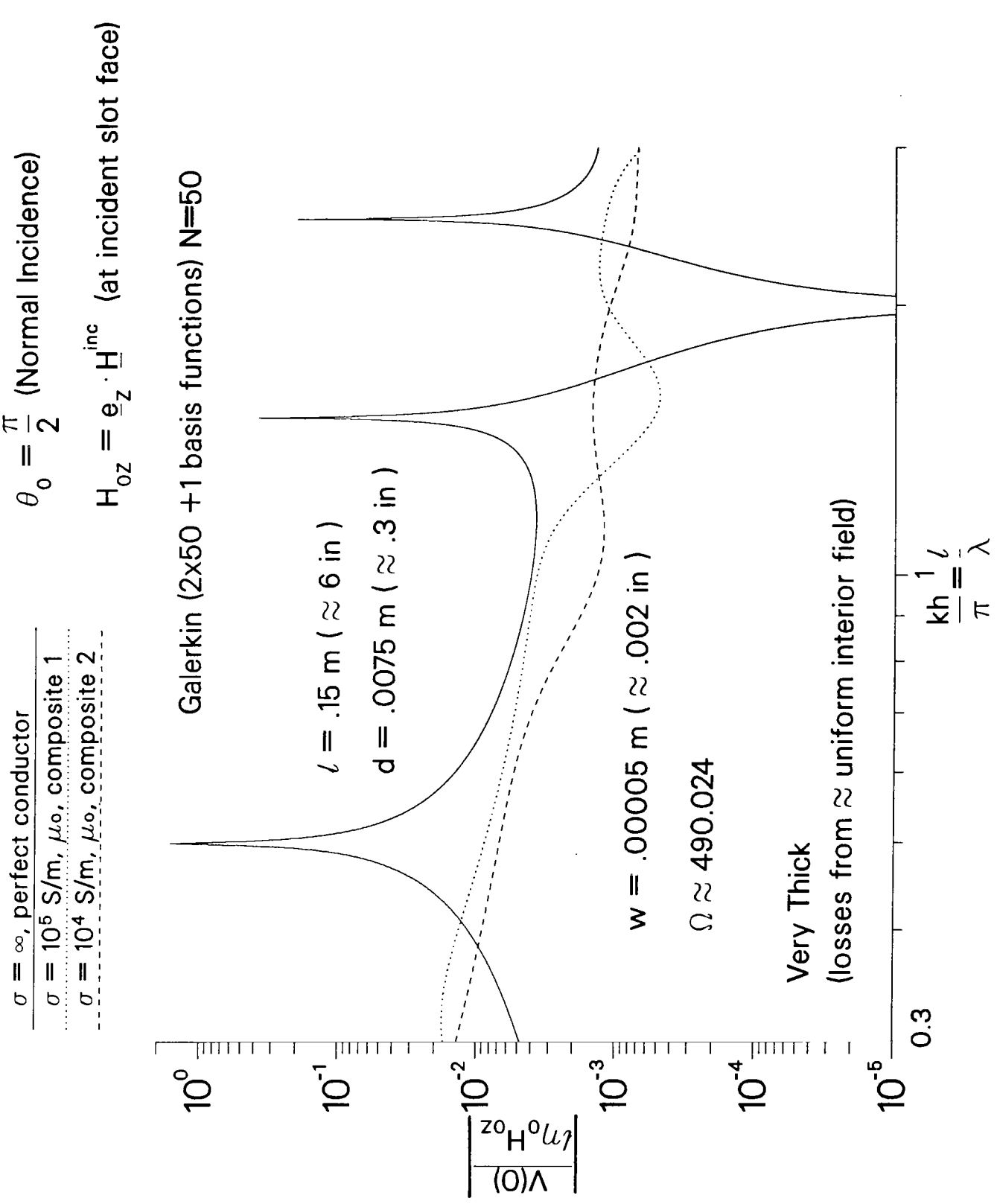

Figure 17. Conductive composite wall material effects are illustrated for a rectangular slot aperture approximately 6 inches in length, 0.3 inches in depth, and 0.002 inches in width. (a) Normalized center voltage magnitude.

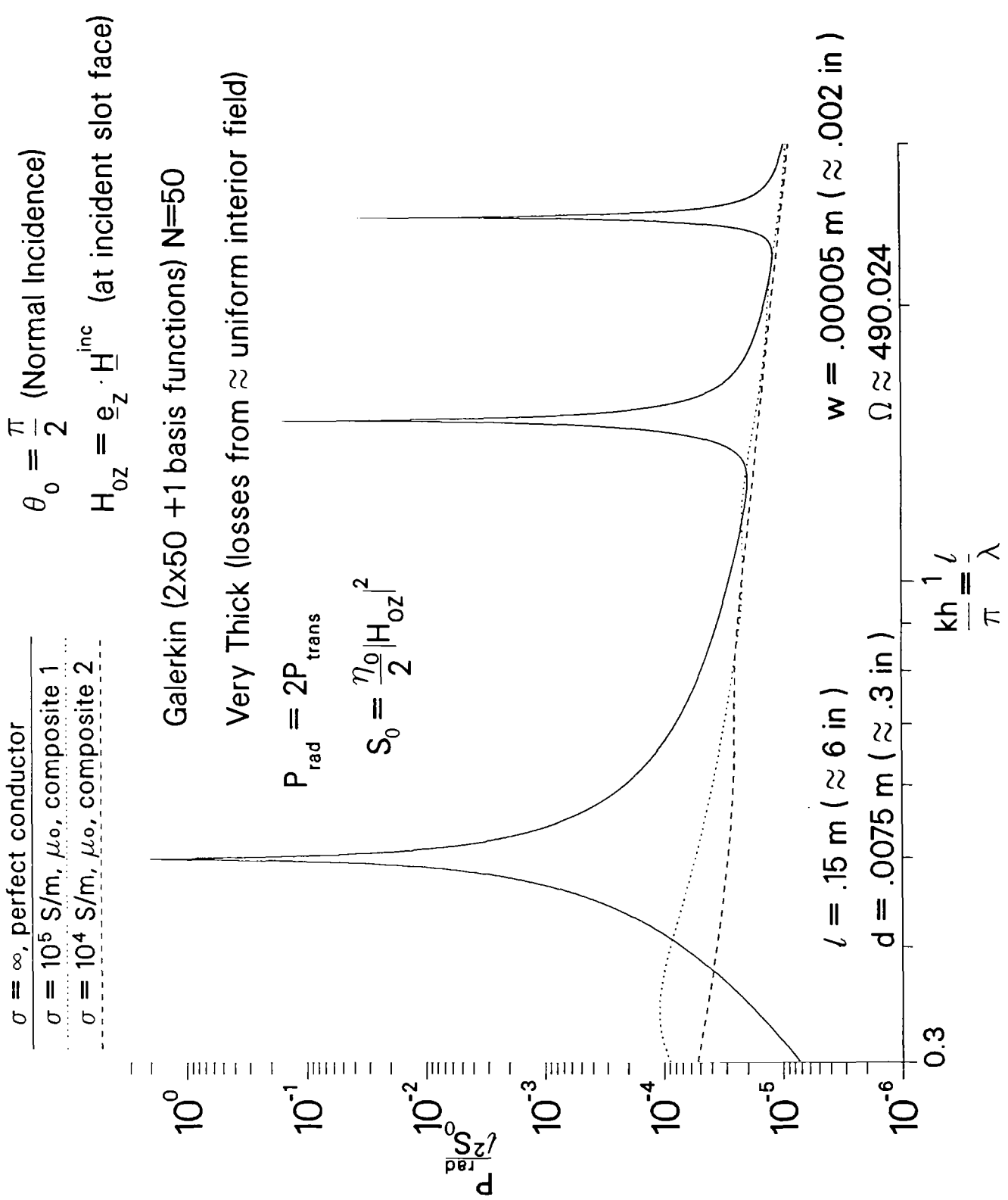

(b) Normalized radiated power.

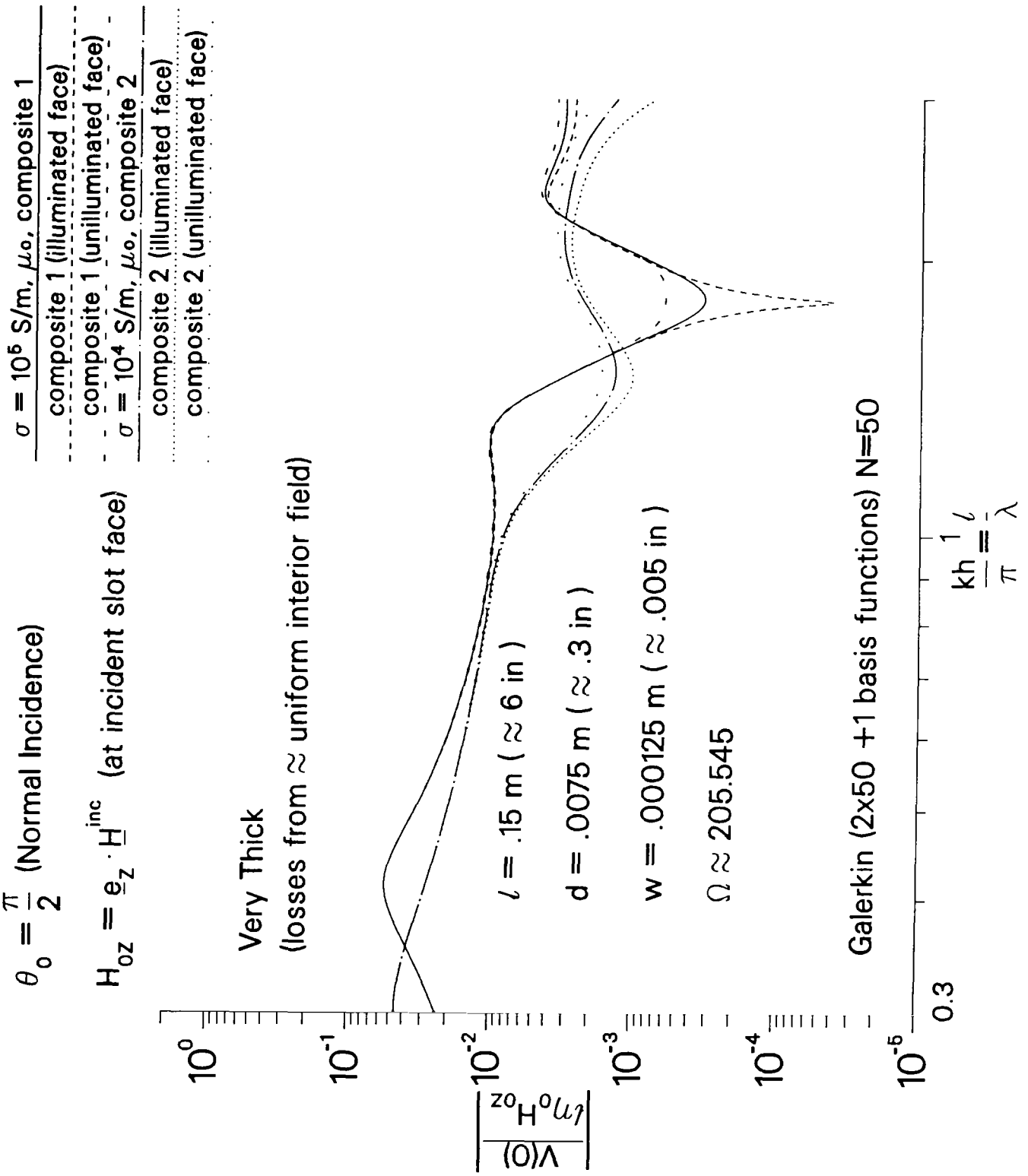

Figure 18. Normalized center voltage magnitude for the geometry of Figure 16. Also shown are the corrections obtained by addition of the odd solution.

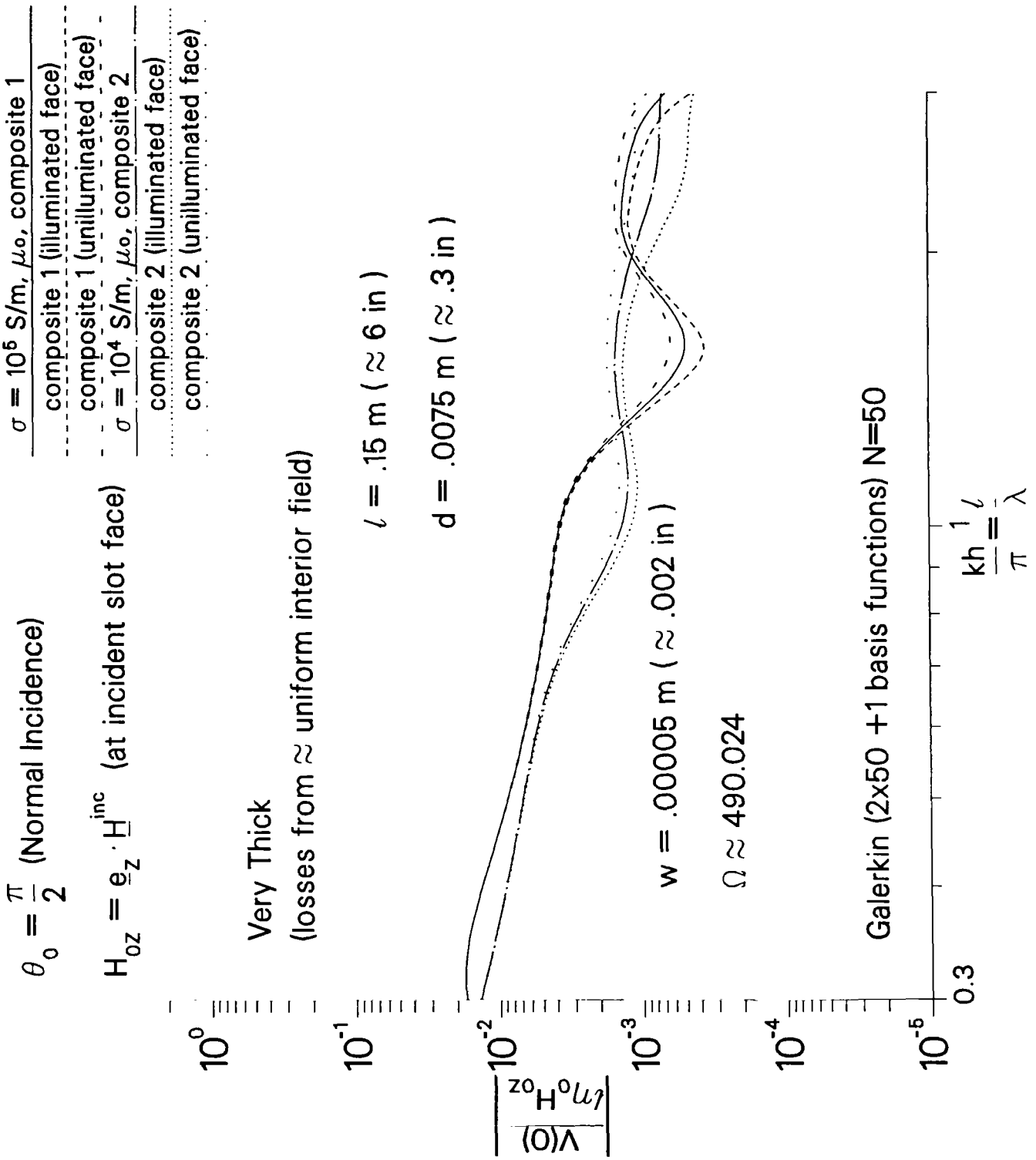

Figure 19. Normalized center voltage magnitude for the geometry of Figure 17. Also shown are the corrections obtained by addition of the odd solution.

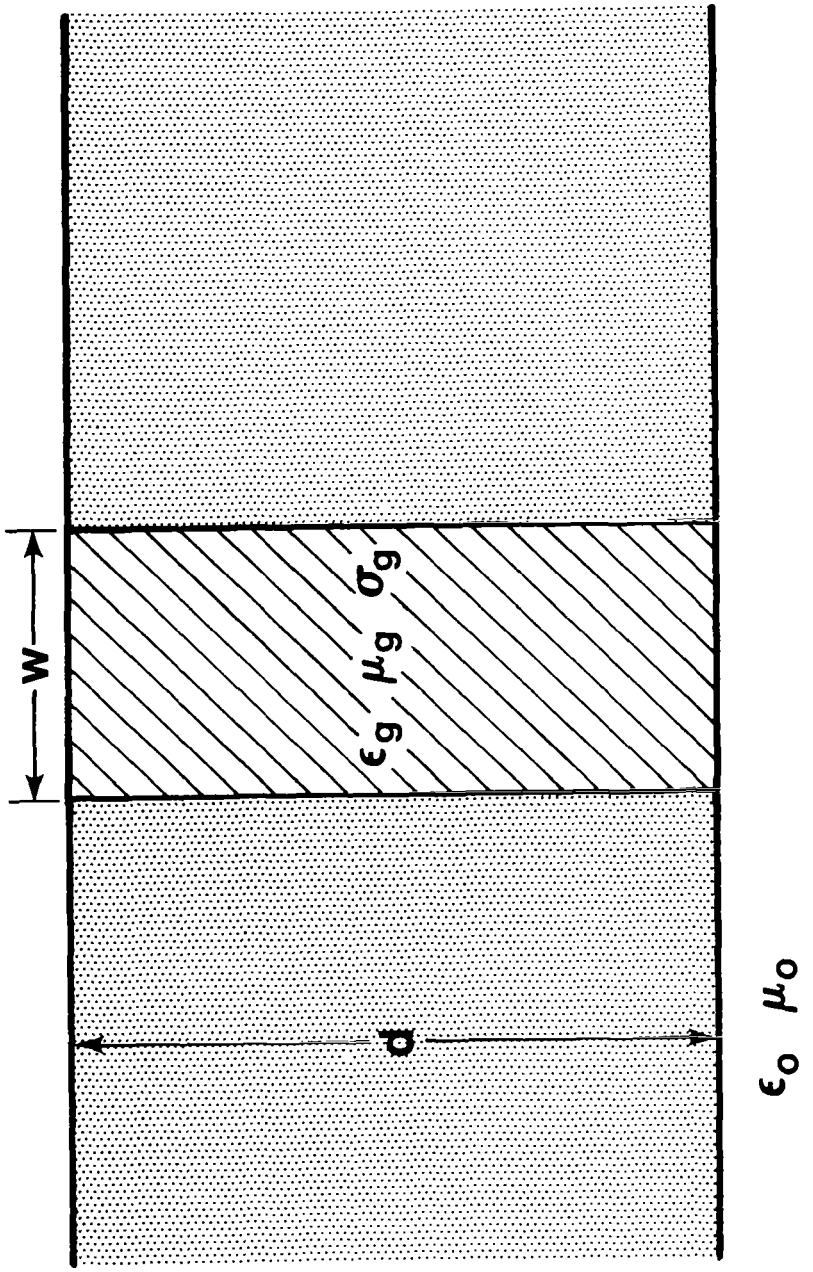

Figure 20. Geometry of rectangular slot aperture with gasket.

radius (53) is again used to include the external elements without the gasket, $L^{o}_{\rho_o}$ and $C^{o}_{\rho_o}$. The inductance and capacitance per unit length are approximately given by

$$\frac{1}{L_{\rho_o}} \approx \frac{2}{\pi\mu_o} \ell n\left[\frac{\rho_o}{w/4}\right] + \frac{d}{\mu_g w} \ , \tag{74}$$

$$C_{\rho_o} \approx \frac{2}{\pi} \epsilon_o \ell n\left[\frac{\rho_o}{w/4}\right] + \frac{d}{w} \epsilon_g \ , \tag{75}$$

where ϵ_g is the gasket electric permittivity. The conductance per unit length can also be approximated as that resulting from a uniform interior field

$$G = G^{intr} \approx \sigma_g \frac{d}{w} \ . \tag{76}$$

Referring to (37) and (38) we obtain

$$\Delta Y_L \approx \frac{1}{-i\omega} \frac{d}{w} \left(\frac{1}{\mu_g} - \frac{1}{\mu_o}\right) \ , \tag{77}$$

$$\Delta Y_C \approx G^{intr} - i\omega \frac{d}{w} (\epsilon_g - \epsilon_o) \ . \tag{78}$$

Figures 21 through 23 show examples of relatively low loss gaskets. Figure 24 shows the effect of the odd problem correction for the geometry of Figure 23.

5. Lossy gasket with air gap without wall loss

Figure 25a shows the geometry of the slot with gasket and air gap. The gasket now has width t. The approximate local circuit model is shown in Figure 25b. The elements are

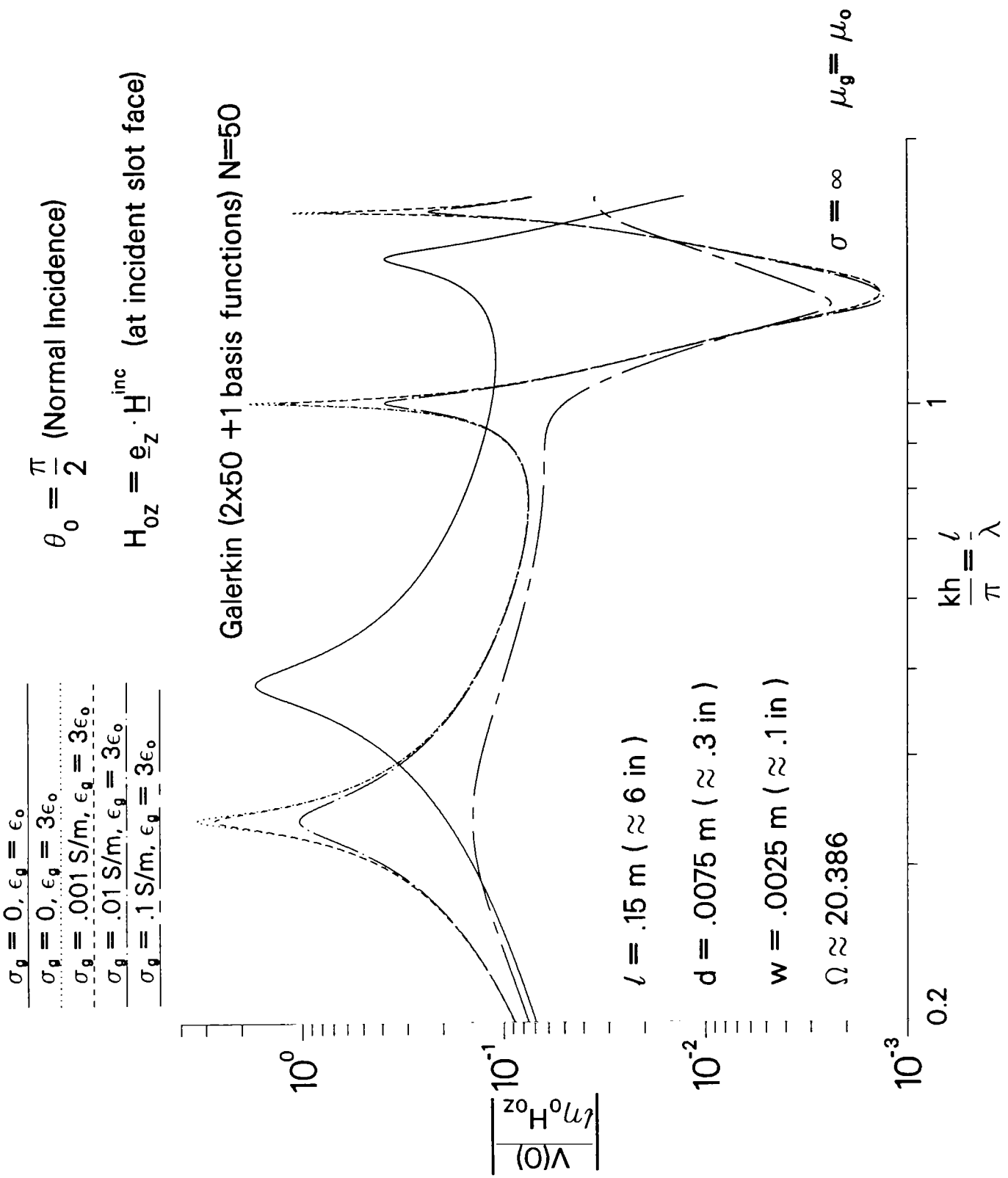

Figure 21. Lossy gasket material effects are illustrated for a rectangular slot aperture approximately 6 inches in length, 0.3 inches in depth, and 0.1 inches in width. (a) Normalized center voltage magnitude.

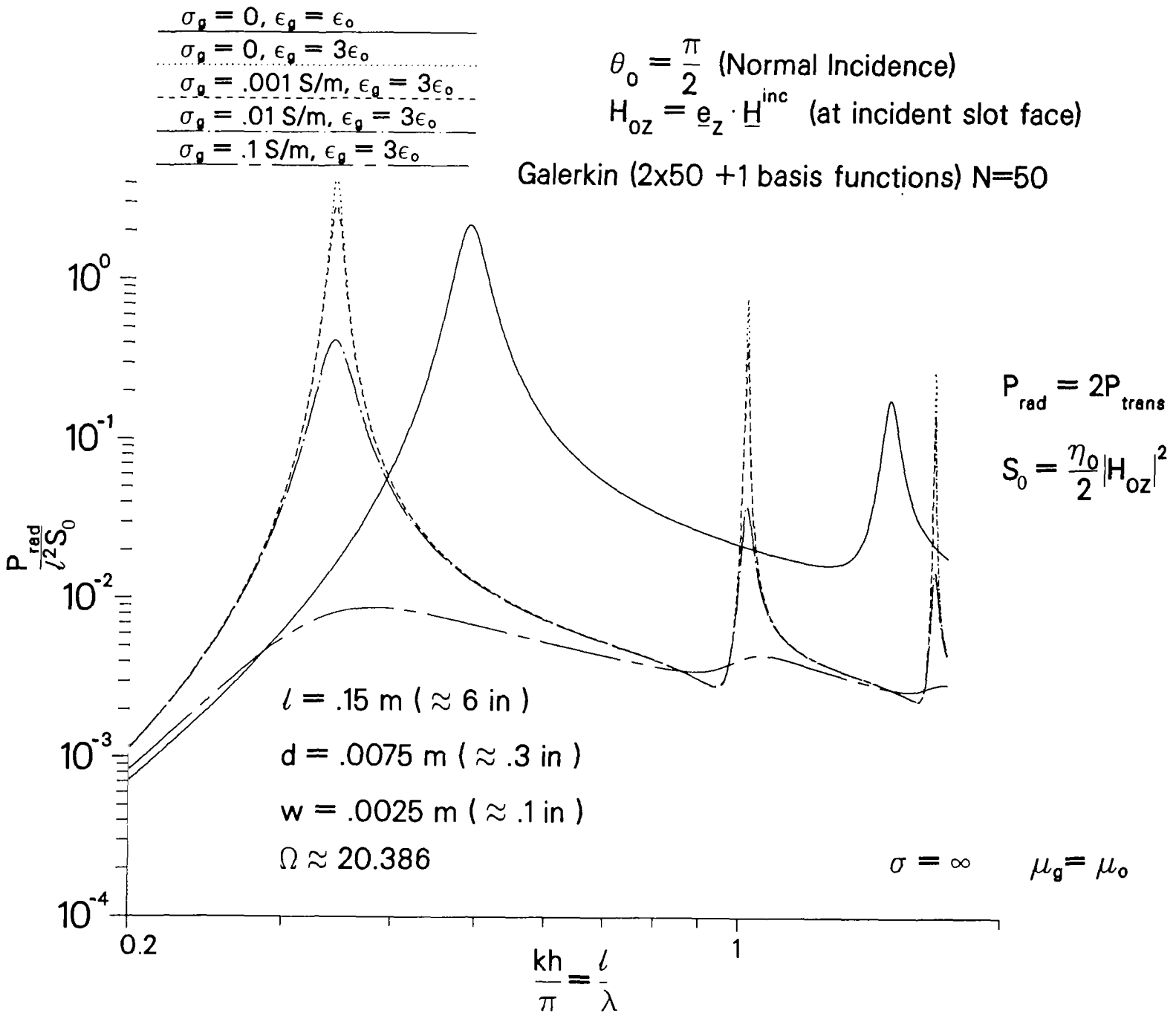

(b) Normalized radiated power.

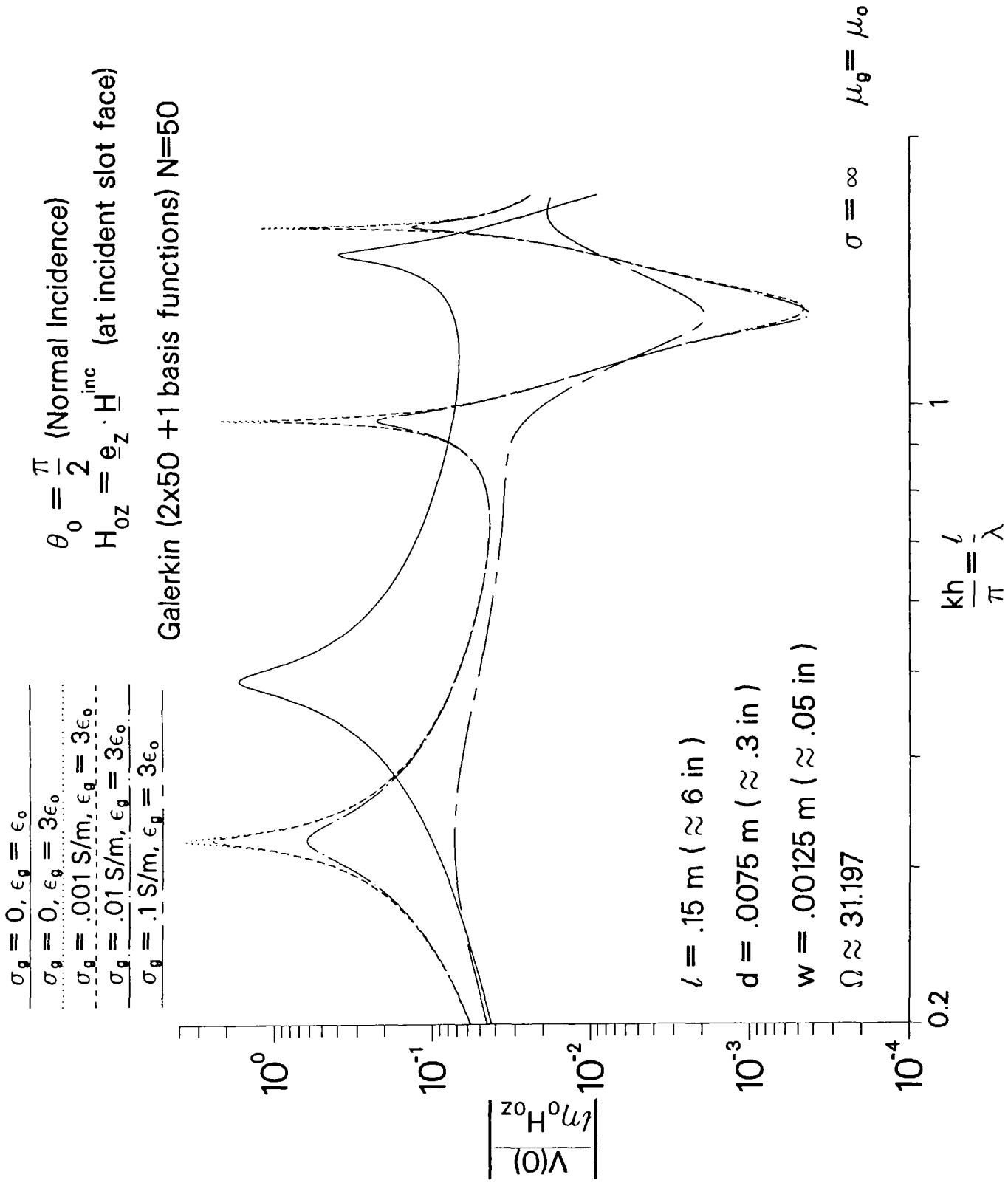

Figure 22. Lossy gasket material effects are illustrated for a rectangular slot aperture approximately 6 inches in length, 0.3 inches in depth, and 0.05 inches in width. (a) Normalized center voltage magnitude.

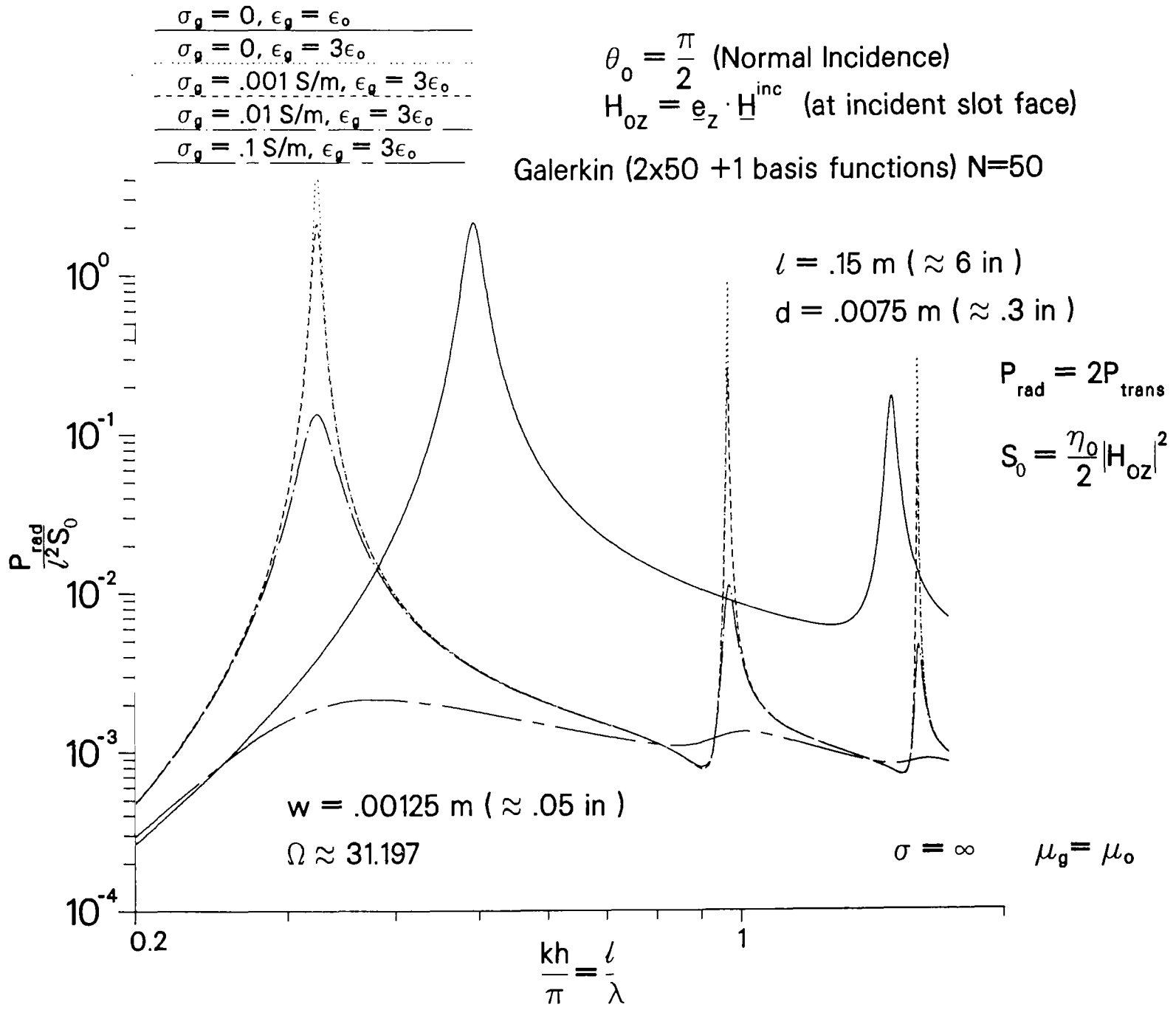

(b) Normalized radiated power.

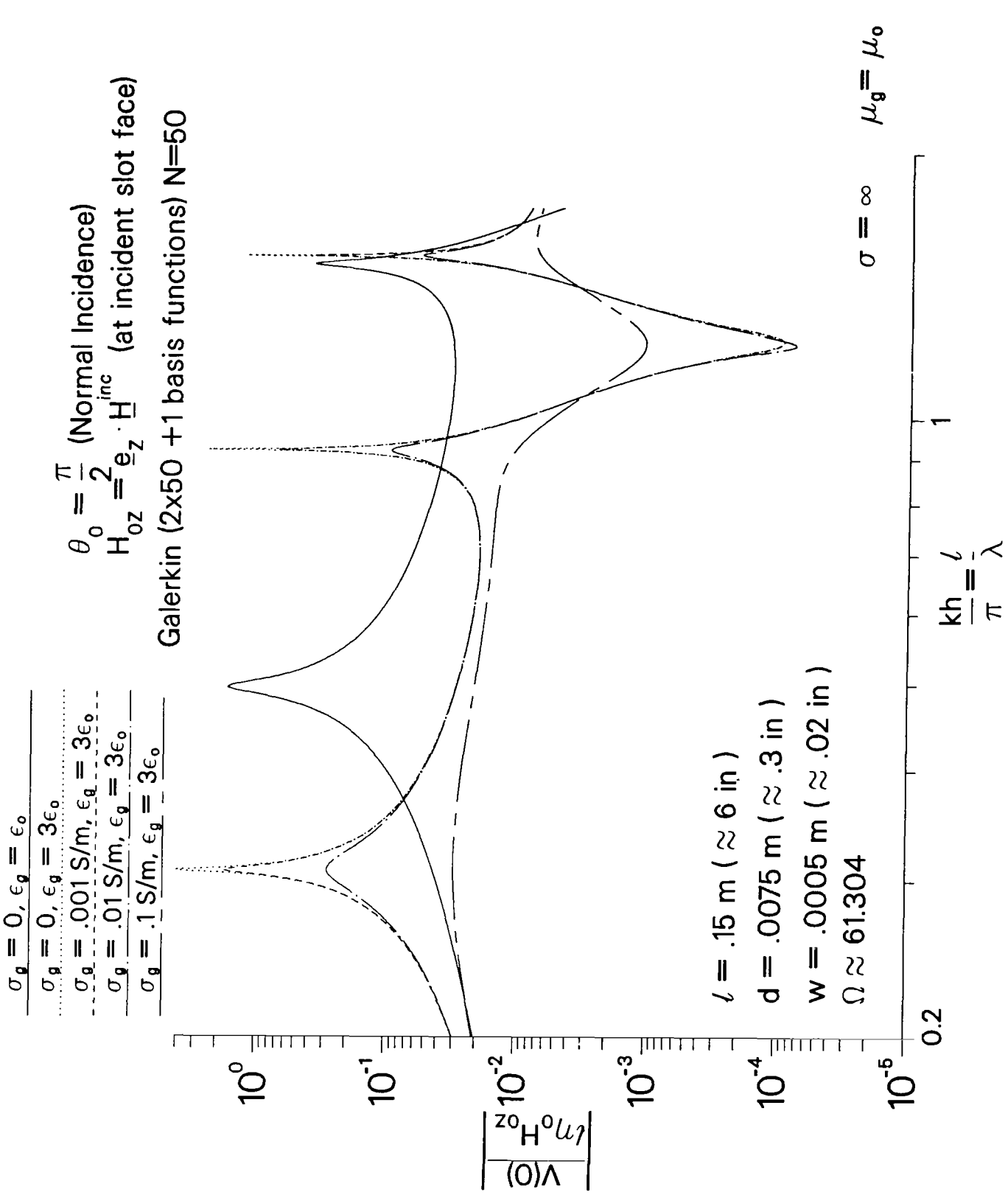

Figure 23. Lossy gasket material effects are illustrated for a rectangular slot aperture approximately 6 inches in length, 0.3 inches in depth, and 0.02 inches in width. (a) Normalized center voltage magnitude.

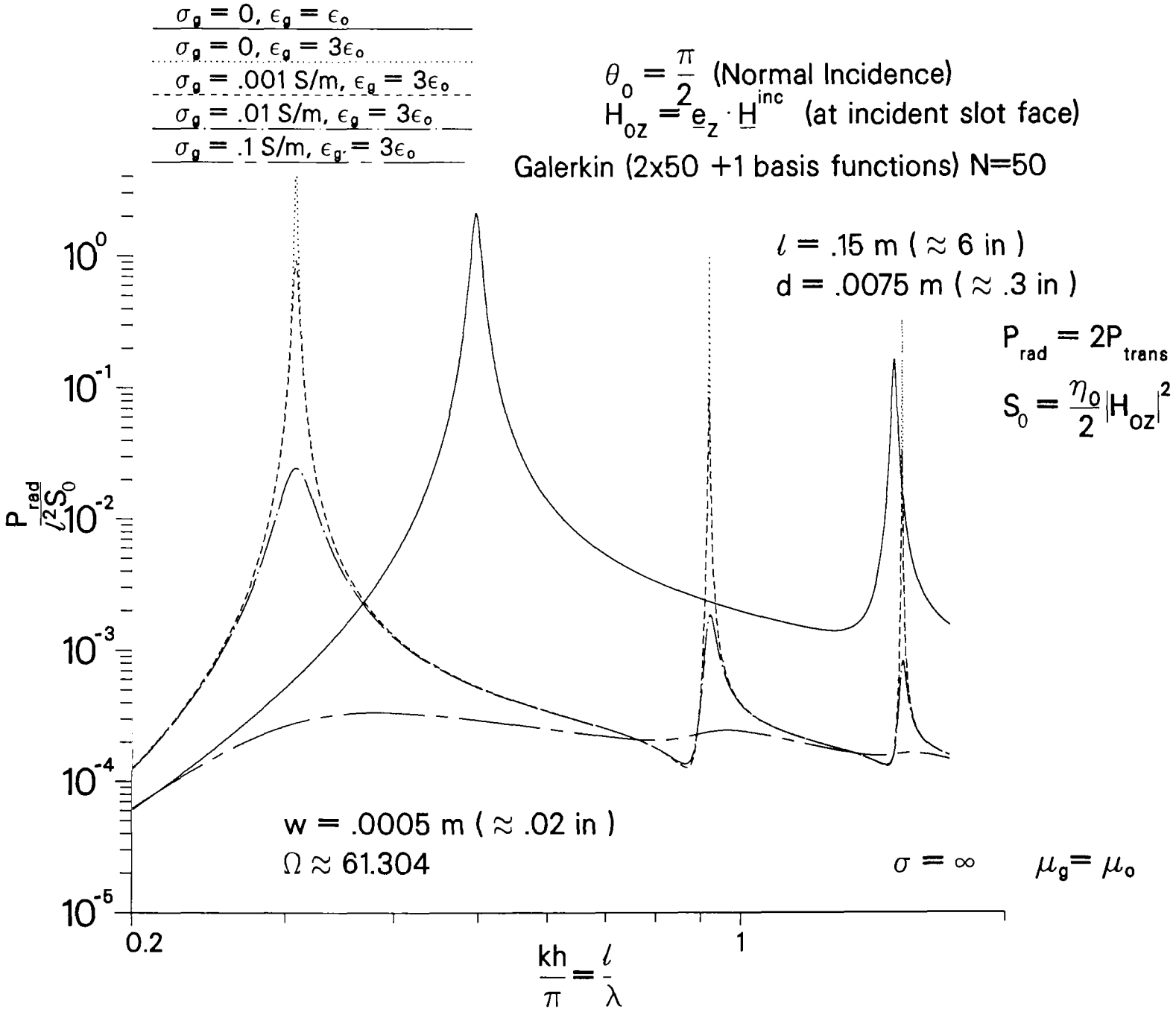

(b) Normalized radiated power.

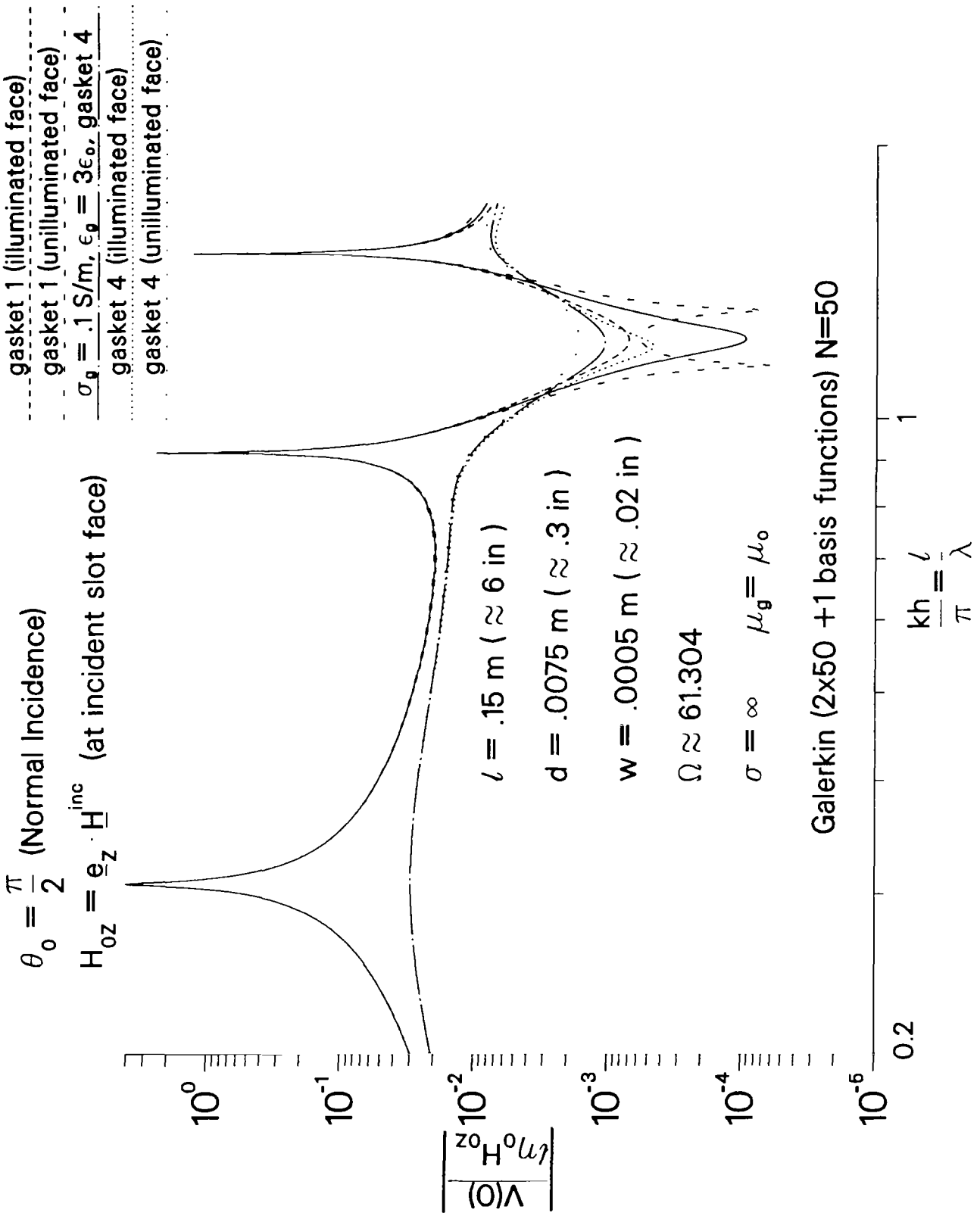

Figure 24. Normalized center voltage magnitude for the geometry of Figure 23. Also shown are the corrections obtained by addition of the odd solution.

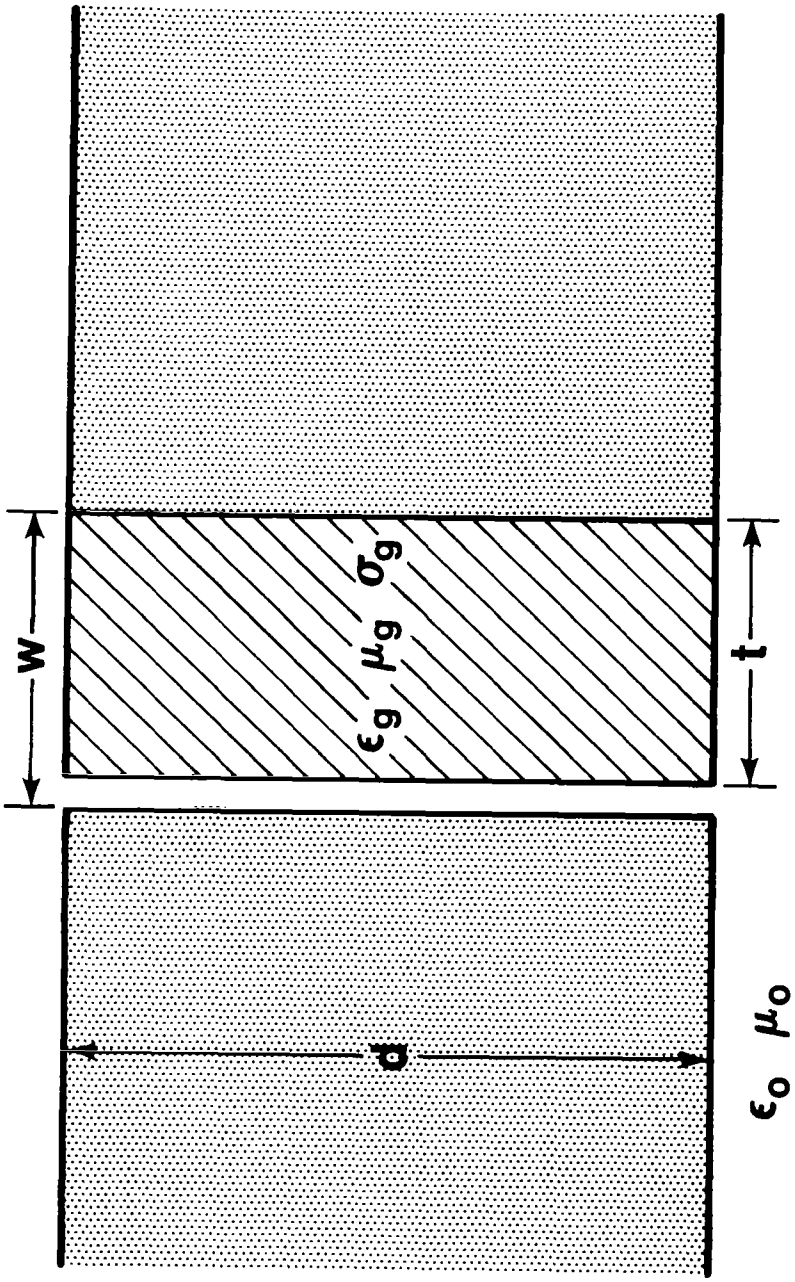

Figure 25. Rectangular slot aperture with gasket and air gap. (a) Geometry.

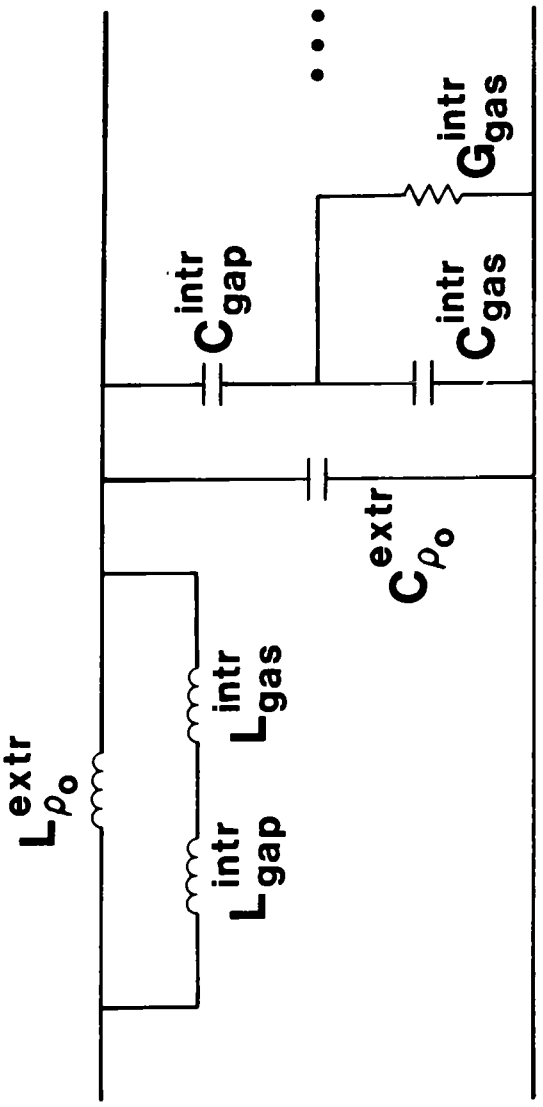

(b) Local circuit model.

$$L_{\rho_o}^{extr} \approx \frac{\pi \mu_o}{2 \ \ell n\left[\frac{\rho_o}{w/4}\right]} \ , \tag{79}$$

$$L_{gas}^{intr} \approx \frac{t}{d} \mu_g \ , \tag{80}$$

$$L_{gap}^{intr} \approx \frac{w - t}{d} \mu_o \ , \tag{81}$$

$$C_{\rho_o}^{extr} \approx \frac{2}{\pi} \epsilon_o \ \ell n\left[\frac{\rho_o}{w/4}\right] \ , \tag{82}$$

$$C_{gas}^{intr} \approx \frac{d}{t} \epsilon_g \ , \tag{83}$$

$$C_{gap}^{intr} \approx \frac{d}{w - t} \epsilon_o \ , \tag{84}$$

$$G_{gas}^{intr} \approx \frac{d}{t} \sigma_g \ . \tag{85}$$

The total admittance per unit length is therefore

$$Y_{\rho_o} = - i\omega C_{\rho_o}^{extr} + \frac{1}{- i\omega C_{gap}^{intr}} + \frac{1}{G_{gas}^{intr} - \frac{1}{i\omega C_{gas}^{intr}}} \ . \tag{86}$$

The total inductance per unit length is found from

$$\frac{1}{L_{\rho_o}} = \frac{1}{L_{\rho_o}^{extr}} + \frac{1}{L_{gas}^{intr} + L_{gap}^{intr}} \ . \tag{87}$$

The approximate equivalent radius (53) can again be used to include $L_{\rho_o}^{o}$ and $C_{\rho_o}^{o}$. The

elements

$$\Delta Y_L = \frac{1}{-i\omega}\left(\frac{1}{L_{\rho_o}} - \frac{1}{L^o_{\rho_o}}\right) , \tag{88}$$

$$\Delta Y_C = Y_{\rho_o} + i\omega C^o_{\rho_o} , \tag{89}$$

thus enter (35) and (36).

Figure 26 gives the results when a small air gap is introduced into the geometry of Figure 22.

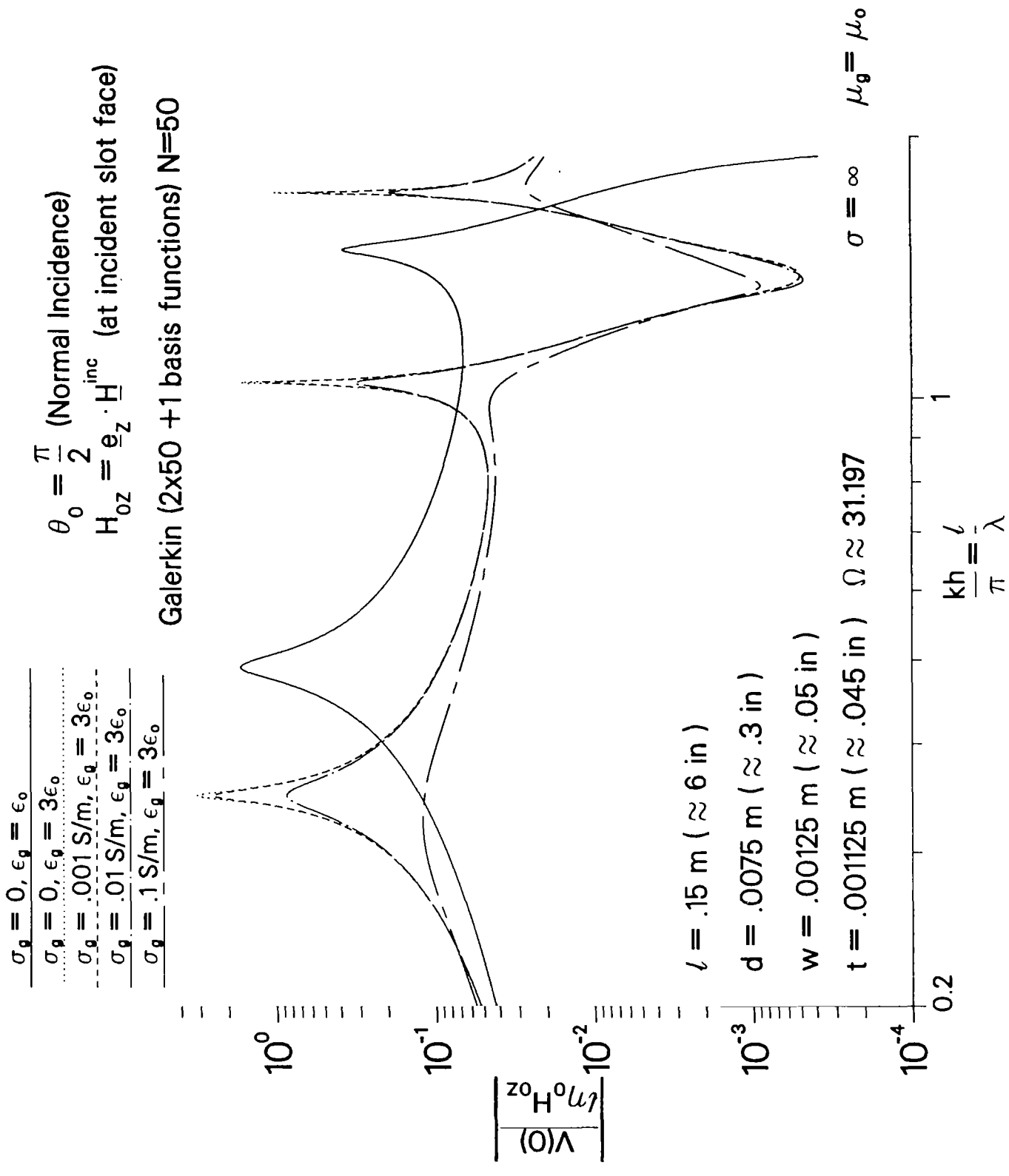

Figure 26. Lossy gasket material effects with an air gap of approximately 0.005 inches in width are illustrated for a rectangular slot aperture approximately 6 inches in length, 0.3 inches in depth, and 0.05 inches in width. (a) Normalized center voltage magnitude.

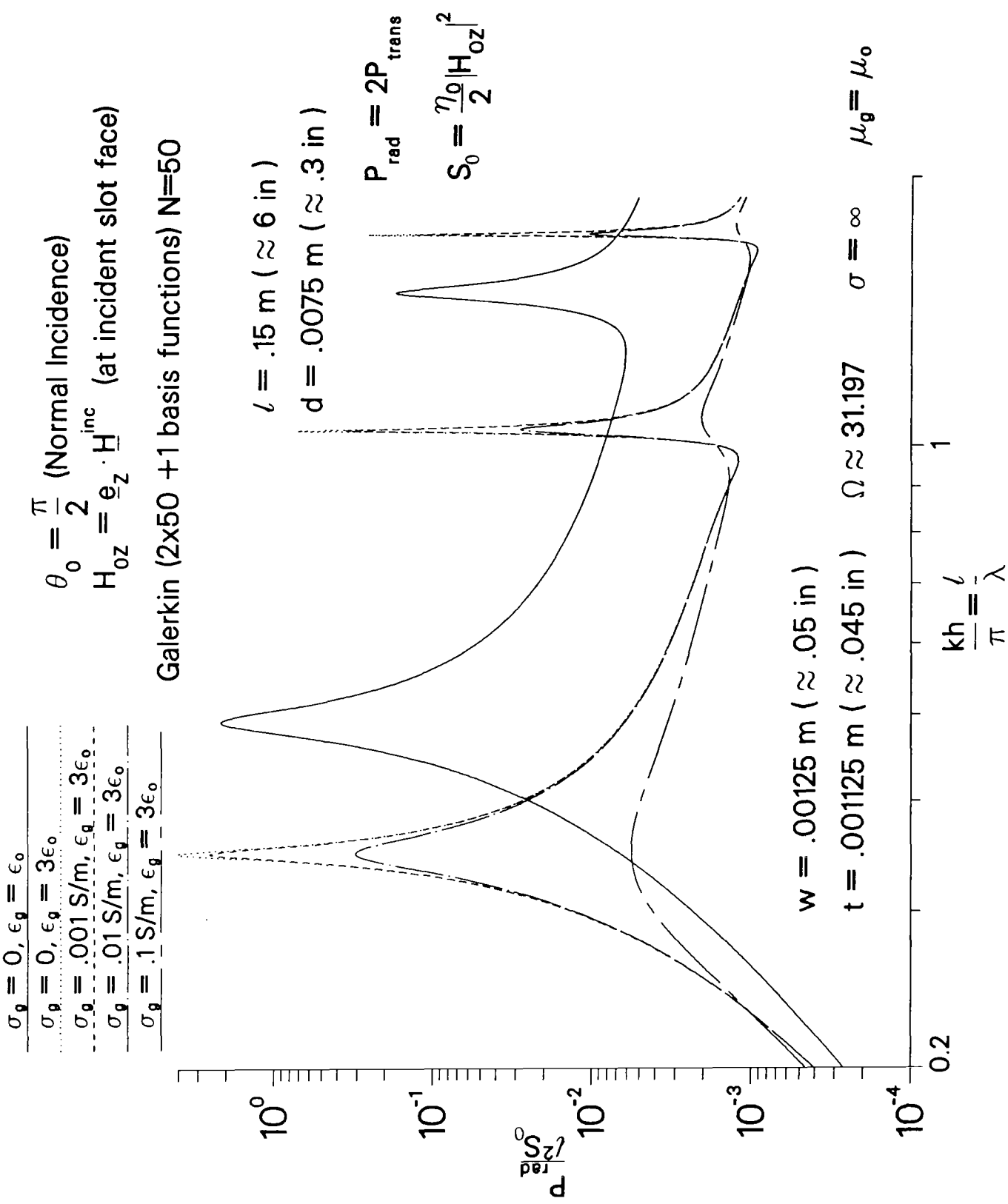

(b) Normalized radiated power.

IV. CONCLUSIONS

A local transmission line – nonlocal antenna model has been introduced that is useful in representing penetration of narrow slot apertures by means of antenna modes. The effects of aperture depth, finitely conducting slot wall materials, and lossy gaskets have been investigated by means of the model.

Large depth–to–width ratios, typical of unintentional joint apertures on systems, give rise to large resonant quality factors. Furthermore, even good metallic conductors result in significantly reduced penetration when typical slot dimensions are used. Gaskets, with relatively small loss tangents, also result in significant reductions in penetration.

It should be pointed out that the fatness parameter Ω is typically large enough in these problems that, in the lossless case without gaskets, simple antenna theories such as Hallén's iteration method [9] and approximations based on the biconical transmission line [10],[11] yield accurate results. In fact, when Ω is very large, a simple transmission line model which includes wall loss and gaskets is easily constructed [8].

A correction to the uniform voltage distribution interior to the rectangular slot aperture is also given. This correction arises from a simple approximate solution to the odd problem in depth. The magnitude of this correction can be used as a gauge of the accuracy of the antenna solution when the depth becomes a significant fraction of a wavelength. A simple model without restrictions on the depth will be discussed in a future paper.

REFERENCES

[1] L. K. Warne and K. C. Chen, "Electromagnetic Penetration of Narrow Slot Apertures Having Depth," AFWL Interaction Notes, Note 464, April 1988.

[2] C. H. Papas, Theory of Electromagnetic Wave Propagation. New York: McGraw–Hill Inc., 1965.

[3] R. W. P. King, The Theory of Linear Antennas. Cambridge, Mass.: Harvard University Press, 1956. Section I.7.

[4] S. A. Schelkunoff, Electromagnetic Fields. New York: Blaisdell Pub., 1963, Chapter 4.

[5] L. K. Warne and K. C. Chen, "Relation Between Equivalent Antenna Radius and Transverse Line Dipole Moments of a Narrow Slot Aperture Having Depth," IEEE Trans. Electromagn. Compat. Vol. EMC–30, No. 3, August 1988.

[6] F. E. Borgnis and C. H. Papas, "Electromagnetic Waveguides and Resonators," Handbuch Der Physik, Vol. XVI, Berlin: Springer Verlag, 1958.

[7] R. E. Collin, Field Theory of Guided Waves. New York: McGraw–Hill Inc., 1960, Chapter 4.

[8] L. K. Warne and K. C. Chen, "Electromagnetic Penetration of Narrow Slot Apertures Having Depth and Losses," Albuquerque: Sandia National Laboratories Report, to be published.

[9] J. D. Kraus, Antennas. New York: McGraw–Hill, Inc., 1950, Section 9–5.

[10] S. A. Schelkunoff and H. T. Friis, Antennas Theory and Practice. New York: John Wiley and Sons, 1952.

[11] E. C. Jordan and K. G. Balmain, Electromagnetic Waves and Radiating Systems. Englewood Cliffs, New Jersey: Prentice–Hall, Inc., 1968, Sections 11.13, 11.14 and Chapter 14.